UNIVERSITY OF NAIROBI

COLLEGE OF BIOLOGICAL AND PHYSICAL SCIENCES

DEPARTMENT OF CHEMISTRY

SYNTHESIS, CHARACTERIZATION AND PHOTOPHYSICAL STUDIES OF NOVEL PORPHYRIN-BASED COMPOUNDS FOR APPLICATION IN PHOTODYNAMIC ANTIMICROBIAL CHEMOTHERAPY (PACT)

BY

JACKLINE NANGILA KHISA

I56/88378/2016

A THESIS SUBMITTED IN PARTIAL FULFILLMENT OF THE REQUIREMENTS FOR THE DEGREE OF MASTER OF SCIENCE IN CHEMISTRY OF THE UNIVERSITY OF NAIROBI

2020

DECLARATION

This thesis is my original work and has not been presented for a degree in any other university. Where other people's work or my own work has been used, this has properly been acknowledged and referenced in accordance with the University of Nairobi's requirements.

Signature ..... Date 10/09/2020

JACKLINE NANGILA KHISA

I56/88378/2016

Department of Chemistry

School of Physical Sciences

University of Nairobi

This thesis is submitted for examination with our approval as research supervisors:

	Signature	Date
Dr. Solomon Derese. Department of Chemistry University of Nairobi P.O. Box 30197-00100 Nairobi	.....	10/09/2020
Dr. Edith K. Amuhaya Department of Chemistry United States International University P.O. Box 14634-00800 Nairobi	Edith Amuhaya	10-9-2020
Dr. Ruth Odhiambo Department of Chemistry University of Nairobi P.O. Box 30197-00100 Nairobi	.....	14/09/2020

DEDICATION

This thesis is dedicated to my parents and my lovely son Richard

ACKNOWLEDGEMENT

First and foremost, I thank God for giving me the strength and determination to complete my Master's research.

I would like to express my sincere gratitude to my hardworking supervisors: Dr. Solomon Derese, Dr. Edith Amuhaya and Dr. Ruth Odhiambo for their patience, guidance and support during the course of my studies. I would like to convey my special regards to Dr. Amuhaya for introducing me to the fascinating realm of porphyrin synthesis. I deeply thank her for the encouragement and suggestions that carried me on through the difficult times and helped to shape my research skills. My gratitude also goes to Dr. Albert Ndakala and Prof. Abiy Yenesew for their continuous support and guidance during my study. I would like to thank the Chemistry Department, University of Nairobi, for giving me the opportunity to study and obtain my Master's Degree. I am grateful to School of Pharmacy at United States International University-Africa (USIU-Africa) for hosting me and providing the necessary facilities that I needed while doing this work. I also appreciate Mr. Eugene, School of Pharmacy for the support and help rendered in ensuring everything in the laboratory was running smoothly. To my colleagues: Mr. Owor, Mr. Oyim, Ms. Murage, Mr. Otieno, Mr. Ivan and Ms. Gathoni, thanks for the support and always being ready to assist. I will always be grateful to my parents, Rose and George Khisa. I can never thank them enough for their unwavering support throughout my studies. You have always been my pillar of strength and my reason to keep going regardless of obstacles. To my son Richard, I am truly blessed to have you in my life. My humble appreciation goes to Mr. Okwaro for the support and care rendered to me during this study. A special thank you to my siblings Everline, Kevin, Frankline and Eli for always walking along side me and putting a smile on my face when things get tough. To my friends, thank you so much for all your encouragements and love throughout this work. You are all highly appreciated. Finally, I express my gratitude to International Development Research Foundation (IDRC), Canada for funding this project, Project Grant Number 108569-001.

ABSTRACT

There are a number of techniques employed to rid microbial contaminants from water. The inefficacy of some of these methods in removing microorganisms in contaminated water, has resulted to increased incidences of water-borne diseases and emergence of antimicrobial resistance by disease causing pathogens. Therefore, there is need to develop new, efficient and convenient methods for combating microbial water contaminants as well as addressing the current problem of antimicrobial resistance. Photodynamic antimicrobial chemotherapy (PACT) is one of the emerging green technologies for water treatment that uses the combined presence of light, oxygen and suitable photosensitizer to generate a reactive oxygen species that is effective against pathogenic microbial organisms. Porphyrins are by far one of the commonly used photosensitizers in PACT. They are stable, tend to absorb in the long wavelength region due to extended π conjugation, and have specific interactions with proteins in cell membrane of bacterial cells. Furthermore, upon irradiation with light of suitable wavelength, porphyrins can produce reactive oxygen species efficient in eradicating bacterial cells. In this study porphyrins were synthesized and their photophysical and antimicrobial activities were measured to determine their suitability in PACT. Free-base 5,10,15,20-tetra(4-bromophenyl) porphyrin (H_2TBrPP**)** and 5,10,15,20-tetra(pyren-1-yl)porphyrin (H_2TPyP) were synthesized using established methods. By inserting zinc, gallium and indium to the free-base of H_2TPyP the corresponding metalloporphyrins were synthesized. The synthesized compounds were purified through column chromatography and characterized on the basis of their mass spectrometry, ^{1}H NMR spectroscopy and elemental analysis. Metallation of the free base H_2TPyP to form a metalloporphyrin afforded improved photophysical properties. There was a bathochromic shift in wavelength of absorption from the parent free base H_2TPyP (λ = 431 nm) to metallated ZnTPyP (λ = 439 nm), GaClTPyP (λ = 440 nm) and InClTPyP (λ = 443 nm). The fluorescence quantum yield in H_2TPyP was higher (ϕ_F = 0.131) than in ZnTPyP (ϕ_F = 0.039), GaClTPyP (ϕ_F = 0.041) and InClTPyP (ϕ_F = 0.017) due to efficient intersystem crossing to the triplet manifold. Upon illumination of the synthesized compounds: H_2TBrPP**,** H_2TPyP, ZnTPyP and InClTPyP, effective dose dependent antimicrobial activity against *Staphylococcus aureus* was exhibited with IC_{50} values of 49.57, 27.89, 12.90 and 16.67 µM, respectively.

Table of content

LIST OF TABLES

LIST OF FIGURES

LIST OF SCHEMES

LIST OF APPENDICES

LIST OF ABBREVIATION

δ	Chemical Shift	LUMO	Lowest Unoccupied Molecular Orbital
^{1}H NMR	Proton Nuclear Magnetic Resonance	MALDI	Matrix Assisted Laser Desorption Ionization
ALA	5-Aminolevulinic Acid	MCD	Magnetic Circular Dichroism
AMR	Antimicrobial Resistance	MS	Mass Spectroscopy
ARB	Antibiotic Resistant Bacteria	*m*	Multiplet
ARG	Antibiotic Resistant Genes	*m/z*	Mass to charge ratio
CDC	Centre for Disease Control	PACT	Photodynamic Antimicrobial Chemotherapy
CHN	Carbon-Hydrogen-Nitrogen	ppm	Parts per million
DCM	Dichloromethane	ROS	Reactive Oxygen Species
DMF	N-N, Dimethylformamide	*s*	Singlet
DDQ	2,3-Dichloro-5,6-dicyano-1,4-benzoquinone	SODIS	Solar Disinfection
DMSO	Dimethyl Sulfoxide	*t*	Triplet
d	Doublet	TLC	Thin Layer Chromatography
GLAAS	Global Analysis and Assessment of sanitation	TOF	Time of Flight
HOMO	Highest Occupied Molecular Orbital	TEA	Triethylamine
IR	Infrared	TFA	Trifluoroacetic acid
IC_{50}	50% inhibition concentration	TMS	Tetramethyl Silane
ISC	Intersystem Crossing	UV-Vis	Ultra Violet Visible
JMP	Joint Monitoring Programme	WHO	World Health Organization

CHAPTER ONE
INTRODUCTION

1.1 Background Information

There are three basic human needs - water, food and shelter - needed by human beings for survival. Human beings use water for various day to day applications including drinking, food preparations and personal hygiene. The consumption of unsafe water impairs health of the consumer through illness, can also result in loss of human life and high cost incurred in treatment of water-borne diseases (WHO, 2003), as a result efforts should be made to ensure water for human consumption is safe.

Over the years, progress has been made to guarantee availability of safe and reliable drinking water. However, according to a World Health Organization (WHO) report in 2017, the joint monitoring program (JMP) estimated that about 2 billion people still have no access to safe water (WHO, 2017a). The various factors that affect the safety of water supplied for consumption can be broadly classified into chemical, radiological and microbial contaminants (WHO, 2017b). Of these, transmission of microbial contaminants through water remains the significant cause of water related illness according to the reported cases of waterborne disease outbreak (Gwimbi *et al*., 2019; Pandey *et al*., 2014; Szãlkai, 2019).

Microbial water contaminants can be classified as: Bacteria, viruses, fungi, and protozoa (WHO, 2017b). These microorganisms are eradicated using antimicrobial agents. However, some microorganisms have acquired resistance from eradication by the same antimicrobial agents that were originally effective in destroying them (WHO, 2014). Emergence of antimicrobial resistance (AMR) is identified to be a major threat to public health worldwide as it weakens the ability of available antimicrobial agents to fight microorganisms and diseases caused by them (Llor and Bjerrum, 2014; Munita and Arias, 2016; Prestinaci *et al*., 2015). Water plays a substantial role in encouraging emergence and spread of antimicrobial resistance (AMR) in microorganisms (Munita and Arias, 2016; Xi *et al*., 2009). This is because it acts as a host for microorganisms, antimicrobial agent residues and facilitates the transfer of antimicrobial resistant microorganisms to other places (WHO, 2014; Xi *et al*., 2009). Water also enables the exchange of resistant genes between bacterial species and provides exposure routes of AMR microorganisms to humans who use the same water for their day to day application (Munita and Arias, 2016; WHO, 2014). In addition to this, water

disinfection through chlorination has been shown to have an unintended consequence of encouraging the emergence of AMR (Jin *et al.*, 2020; Neth *et al*., 2017). This is attributed to the fact that antimicrobial agents such as antibiotics which could find their way into water sources, may combine with the disinfectant chlorine, forming transformation products that has been shown to have stronger antimicrobial properties (Neth *et al*., 2017). Presence of these stronger antimicrobial agents in the environment (water or soil) in non-therapeutic concentration provides a suitable platform for the emergence of resistant strain of microorganisms and transfer of resistant genes (Neth *et al*., 2017). This weakens the ability of the originally effective antimicrobial agents to fight diseases (Jin *et al.*, 2020; Munita and Arias, 2016; Neth *et al*., 2017).

The commonly used methods in improving water safety by managing pathogenic microbial organisms in water include: Boiling, chlorination and UV irradiation (WHO, 2017b). Despite these methods being used there is still about 2 billion people in the world have no access to improved water (WHO, 2017a). As mentioned above, resistance of microorganisms to the originally effective antimicrobial agents is a significant health problem (Llor and Bjerrum, 2014; Prestinaci *et al*., 2015) and chlorination one of the commonly used methods in improving the safety of water has been shown to be having potential effect on health by encouraging the emergence of antimicrobial resistant microorganisms (Neth *et al*., 2017). Therefore, there is need to develop other efficient and convenient methods for managing microbial contamination in water (Jori and Brown, 2004; WHO, 2014). Photodynamic antimicrobial combination therapy (PACT) has proven to be a very promising approach for efficient inactivation of pathogenic microorganisms in water. This technique uses the combined presence of a suitable photosensitizer, light and molecular oxygen to produce reactive oxygen species which are lethal to microbial cells (Carvalho *et al*., 2007; Tavares *et al.*, 2010). Preliminary studies have shown this approach to be effective *in-vitro* against various strains of microbial organisms such as bacteria (Carvalho *et al*., 2007) and no incidence of photoresistance in bacteria has been reported even after multiple treatments (Tavares *et al.*, 2010).

Porphyrin compounds are by far one of the commonly used photosensitizers in PACT. This is because they are stable, can chelate different metal ions and they absorb within the visible area of the spectrum. Additionally, porphyrin properties can be modified by attaching functional groups

at the *meso* and beta position of the porphyrin macrocycle (Rastogi and Dwivedi, 2006; Vicente, 2001). Hence in this project, *meso*-tetrakis(4-bromophenyl)porphyrin and *meso*-tetrakis(pyren-1-yl)porphyrin free-base were synthesized. By inserting metal zinc, gallium and indium to the free-base of *meso*-tetrakis(pyren-1-yl)porphyrin the corresponding metalloporphyrins were synthesized. Their photophysical and antimicrobial properties were determined for potential application as photosensitizers in PACT.

1.2 Statement of the Problem

The presence of microbial contaminants in water continues to pose a great danger to human and animals health due to their ability to transmit infectious and potentially life threatening diseases (Bharadwaj and Sharma, 2016; Tanih, 2014; WHO, 2017a). Some of the commonly used water de-contamination methods such as boiling, chlorination and UV-Irradiation, are however time consuming, expensive, unreliable and encourage incidences of antimicrobial resistance (Neth *et al*., 2017; WHO, 2014). For this reason, water-borne diseases and incidences of antimicrobial resistance is becoming a major health problem not only in third world countries, but also in more economically developed countries as well (WHO, 2014). Worldwide it is estimated that 2 billion people have no access to safe water and 485, 000 diarrheal deaths each year are caused by consumption of contaminated water (WHO, 2017a). Therefore, the need to develop other efficient and convenient methods that can help improve management of microbial water contaminants becomes a priority.

1.3 Objectives

1.3.1 General Objective

The general objective of this study was to synthesize novel *meso*-(metallo)porphyrins and determine their photophysical and antimicrobial properties.

1.3.2 Specific Objectives

The specific objectives were: -

1. To synthesize and characterize *meso*-tetrakis(4-bromophenyl)porphyrin and *meso*-tetrakis(pyren-1-yl)porphyrin free-base and the corresponding zinc, gallium and indium metalloporphyrins.
2. To determine the photophysical properties of the porphyrin derivatives.

3. To determine the antimicrobial properties of the synthesized porphyrin derivatives against *Staphylococcus aureus*.

1.4 Justification and Significance

In July 2010, U.N. General Assembly through resolution A/RES/64/292, recognized that access to safe water is a basic human right. While substantial progress has been made to guarantee accessibility to safe and reliable water, it is estimated that billions of people still do not have access to this basic need (WHO, 2017a; WHO, 2019). Worldwide, it's approximated that one in three people cannot access safe water and microbial water contamination remains to be a major water quality concern (CDC, 2014a; Szãlkai, 2019; WHO, 2019). So as to achieve Kenya Vision 2030 and Sustainable Development Goal (SDG 6) of ensuring universal accessibility to safe, reliable and affordable water by 2030, there is need to explore new approaches aimed at managing microbial water contamination (Karumathil *et al.*, 2014; Neth *et al*., 2017; U.N. Water, 2019). Studies have shown that PACT is a promising approach for management of microbial organisms while avoiding incidences of antimicrobial resistance (Carvalho *et al*., 2007; Tavares *et al.*, 2010). With the use of efficient photosensitizer, the activity of PACT against various microbial organisms can improve tremendously. It is proposed that pyrene containing porphyrins have enhanced singlet oxygen generating ability (Mananga, 2017). Furthermore, extending the π conjugation through presence of pyrene groups results to a bathochromic shift in absorption wavelength (Detert *et al.*, 2010). Metalation of the porphyrin promotes intersystem crossing to the triplet state (Ji *et al.*, 2015; Knör and Strasser, 2002) enhancing production of singlet oxygen and free radicals which are the effective toxic agents in PACT (Foote, 1991; Porfirinas and Fotodin, 1996). To address this in this study, *meso*-tetrakis(4-bromophenyl)porphyrin and *meso*-tetrakis(pyren-1-yl)porphyrin free-base as well as the corresponding zinc, gallium and indium metalloporphyrins were synthesized and characterized. Photophysical and antimicrobial studies of the synthesized compounds were evaluated to determine their potential use as photosensitizers in managing microbial water contaminants.

CHAPTER TWO
LITERATURE REVIEW

2.1 Introduction

Water is an essential commodity needed by man for various day to day activities for drinking, food preparations and personal hygiene. However, water supplied for human consumption could be a carrier of various disease-causing organisms pausing a significant health risk to its consumers, Hence, the need to ensure right quality of water supplied for consumption becomes a priority. This chapter covers the guidelines used to describe water quality, common water disinfection approaches and Photodynamic Antimicrobial Chemotherapy (PACT) as an alternative approach for water decontamination. Additionally, this chapter discusses porphyrins as photosensitizers in PACT and laboratory methods used for the synthesis of these porphyrin compounds.

2.2 Guidelines to Describe Water Quality

There are various aspects of water that are put into consideration when describing the quality of water supplied for human consumption which can broadly be simplified as radiological, chemical and microbial water quality (WHO, 2017b).

2.2.1 Radiological Water Quality

Radiological water contaminants are undesired radioactive compound that is present in water used for human consumption. These radioactive compounds contain unstable atoms that can emit ionizing radiation such as gamma rays, alpha and beta particles (EPA, 2017). In living cells, the ionizing radiations emitted by radiological contaminants are able to kill cells and cause cell mutation that could thereafter become cancerous (WHO, 2017b; EPA, 2017). Some of the common radiological water contaminants are uranium, plutonium, and cesium (WHO, 2017b).

2.2.2 Chemical Water Quality

There are many chemicals that exist in the universe. Nonetheless, it has been shown that only a small number of chemicals when present in excess amounts in water supplied for human consumption can cause extensive health effect (U.N. Water, 2019; WHO, 2017b). Additionally, experience shows that presence of most chemical contaminants in water alters its taste, appearance and odor making it unpalatable. The chemical water contaminants can be grouped into organic pollutants such as fertilizers and heavy metals such as lead, cadmium and mercury (EPA, 2017; WHO, 2017b). Removal of these chemical contaminants from water is actually an expensive and

sometimes impossible process hence efforts need to be made to avoid chemical waste discharges in water. Common sources of chemical water contaminants are industrial waste discharge, agricultural chemical run-offs and fuel discharge (WHO, 2017b).

2.2.3 Microbial Water Quality

Water supplied for human consumption has the potential of transporting microbial pathogens to a great number of its consumers (WHO, 2017a). Pathogens are microorganisms that have the potential of causing diseases to human beings if ingested through food, drinking water or physical contact with contaminated water. Transmission of pathogenic microorganisms by drinking water remains a significant cause of illness according to the reported cases of water-borne disease outbreak (Gwimbi., *et al*., 2019; Pandey *et al*., 2014; Szãlkai, 2019). Hence, priority needs to be given in developing water sources free from microbial water contaminants. The microbial water contaminants can be classified as: Bacteria, viruses, fungi and protozoa (WHO, 2017b). Among the four, bacterial water contamination has been identified as a leading cause of water-borne disease outbreak (Gwimbi *et al*., 2019; Pandey *et al.*, 2014; Yoder *et al*., 2008).

2.3 Bacteria

Bacteria are single celled, pathogenic microscopic organisms commonly found in water sources supplied for human consumption (Raven and Johnson, 2002). They are increasingly becoming resistant to the originally effective antimicrobial agents and medical procedures which depend on these agents will become impossible to manage in the near future due to the emergence of resistant strain (Munita and Arias, 2016). Bacteria can be differentiated based on their four basic shapes as *Bacilli*, *Cocci*, *Vibrio* and *Spirillus* (spirilla). Figure 2.1 below shows the four basic shapes of bacteria.

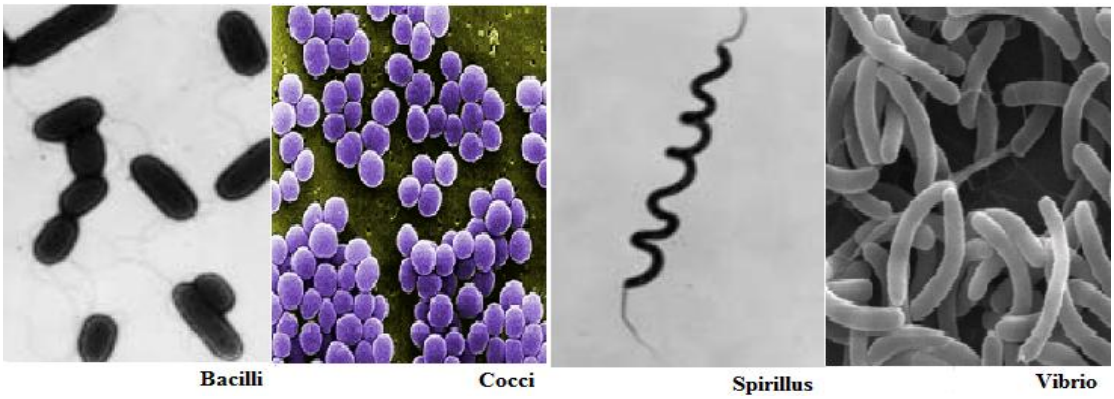

Figure 2.1: Diagram showing classification of bacteria based shape (Raven and Johnson, 2002)

Additionally, bacteria can also be differentiated into gram positive and negative based on gram staining test (Jori and Brown, 2004). As shown in Figure 2.2 below, both bacteria have peptidoglycan layer in their outer envelope. However, on comparison the peptidoglycan layer in gram positive bacteria is thicker (Jori and Brown, 2004). The crystal violet dye used in gram staining test is trapped by the thick peptidoglycan layer making the bacteria appear purple. Gram negative bacteria in contrast has less peptidoglycan hence does not trap the crystal violet dye, the bacteria stains red. The gram negative bacteria instead has a multi layered outer envelope having a cell wall which is absent in gram positive bacteria (Raven and Johnson, 2002).

Figure 2.2: Diagram showing difference in outer envelope between gram positive and negative bacteria (Jori and Brown, 2004).

2.3.1 Common pathogenic bacteria in water

The presence of bacterial pathogens in water renders it unfit for human consumption as it has been proven to cause a wide range of life threatening diseases (Tanih, 2014; Bharadwaj and Sharma, 2016). In this section *Escherichia coli* and *Staphylococcus aureus* are discussed as the common bacteria whose presence in water is one of the root cause of various diseases and infections.

2.3.1.1 *Escherichia coli*

Rod-shaped *Escherichia coli* is a gram negative bacterium that belongs to the genus *Escherichia* (Sekwadi *et al*., 2015; Bharadwaj and Sharma, 2016). This bacteria commonly occurs in the gastrointestinal tract of humans and animals. *E. coli* can be expelled to the environment through fecal matter and thereafter find its way to water supplied for human consumption through rainfall, snow melt and precipitation (CDC, 2014b; Sekwadi *et al*., 2015). If present in water, the bacteria has been reported to cause life threatening diseases to humans worldwide. It could lead to severe abdominal pain, fever, acute diarrhea that could turn bloody within 24 hours, septicemia, mastitis, gram negative pneumonia and urinary tract infections (Bharadwaj and Sharma, 2016; CDC, 2014b). Among children, elderly and persons with compromised immune system, consumption of water contaminated by this bacteria can cause more severe health risk (Bharadwaj and Sharma, 2016; WHO, 2018; CDC, 2014b).

2.3.1.2 *Staphylococcus aureus*

Staphylococcus aureus is a gram positive bacteria (Chang *et al.*, 2013). This bacteria, discovered in the 1880's by Dr. Ogstrong, is now one of the main human bacterial pathogens that has in the recent years attracted the interest of many researchers (Chambers and Deleo, 2010). This is due to its ability to become resistant to the commonly used antibiotics posing a great risk to human and animal health (Chang *et al.*, 2013). The bacteria are prevalent in the environment (air, water and soil) and in human nose and skin (Chambers and Deleo, 2010; Chang *et al.*, 2013; Lowy, 2003). When present in domestic water supplies there is need for concern as it could find its way to food through food preparation practices and drinking water. This results to food related health issues (*Staphylococcal* food poisoning) by producing *Staphylococcal* enterotoxins. *Staphylococcal* food poisoning has a rapid onset of severe symptoms some of which include vomiting, stomach upset, loose bowels and dehydration (Mark and Ramon, 1980; Pinchuk *et al.*, 2010).

Additionally, due to its invasiveness and ability to take advantage of the compromised immune system of the host, *S. aureus* bacteria also causes non-food related diseases such as minor skin infections, abscesses, septicemia and meningitis (Grinholc *et al*., 2007; Chang *et al.*, 2013). In healthcare facilities, it is considered a significant health problem as it is a leading cause of infections acquired in hospitals (Chambers and Deleo, 2010; Chang *et al.*, 2013). Because of this, new approaches for the control of this bacteria have become necessary (Lowy, 2003; Chambers and Deleo, 2010)**.** In this study, the porphyrin derivatives synthesized were studied for their potential in the management of *Staphylococcus aureus* bacteria.

2.3.2 Antimicrobial Resistance

Resistance to antimicrobial agents is one of the main challenges in effective management of pathogenic microorganisms. Antimicrobial resistance is developed when microorganism acquire resistance from destruction by the same antimicrobial agents that were originally effective in destroying them (WHO, 2014). Resistant microorganisms have been found in various water sources, both treated and untreated, supplied for human consumption (Yuan *et.al.,* 2015). The transfer of these AMR to humans leads to longer treatment methods through the use of advanced and expensive antibiotics, longer stays in hospitals and increased risk of mortality due to lack of response to antibiotics during treatment (Llor and Bjerrum, 2014; Munita and Arias, 2016; Prestinaci *et al*., 2015).

Antimicrobial resistance can occur naturally when bacteria replicate themselves inappropriately or resistant genes are exchanged between them (Jin *et al.,* 2020). However, this process is enhanced through uncontrolled use of antimicrobial agents by humans (WHO, 2014). In addition to this, presence of antimicrobial agents in the environment at non-therapeutic concentrations provide a suitable platform for microorganism to coexist with antimicrobial agent hence the microorganism is able to develop mechanisms to survive in the harsh environment (Jin *et al.,* 2020; Munita and Arias, 2016; Neth *et al*., 2017). As a result, this weakens the available antimicrobial agents' ability to fight diseases as it encourages the emergence of resistant microorganisms (Munita and Arias, 2016; Neth *et al*., 2017).

2.4 Water Disinfection Approaches

Some of the commonly used methods in managing microbial contaminants in the water sources include: Boiling, Chlorination and UV irradiation (WHO, 2017b).

2.4.1 Boiling

Boiling employs use of heat for the destruction of microbial organisms in water (WHO, 2015). The recommended procedure is raising the temperature of water so that boiling is achieved, allowing the boiled water to cool then protecting it from contamination during storage. It is one of the frequently used methods in various households, however, failure to raise temperature of water to boiling may reduce its effectiveness in managing microbial contaminants as some pathogenic microorganisms may not be destroyed (WHO, 2015; WHO, 2017b). Additionally, it is expensive in terms of fuel, not suitable for large scale application and has increased risk of injuries from getting burnt (WHO, 2017b).

2.4.2 Chlorination

Chlorination is currently one of the most commonly used methods in water disinfection that employs the use of chemical chlorine. It is a fast, less expensive method for water disinfection, however, it has limited activity against biofilms, may not be able to inactivate some protozoa and traces of chemical by product of chlorination may remain in the water (WHO, 2003). Chlorination use in water disinfection has also been shown to be having potential negative effect on health by encouraging the emergence of antimicrobial resistant microorganisms (Jin *et al.,* 2020; Neth *et al*., 2017). This is attributed to the fact that chlorine use in water disinfection may promote

development of new strain of antimicrobial compounds that could then be released to the environment in non-therapeutic concentrations, where they could potentially promote antimicrobial resistance (Karumathil *et al.*, 2014; Neth *et al*., 2017).

2.4.3 UV Irradiation

UV light irradiation technology allows water in a vessel to be exposed to the radiation at germicidal wavelength of about 254nm to inactivate microbial pathogens in water (WHO, 2017b). This technology has limited application as it is quite costly, dependent on electricity and has limited application especially in decontaminating colored water due to restricted UV radiation penetration (WHO, 2017b). In developing countries, UV irradiation water treatment is applied through Solar disinfection (SODIS), whereby contaminated water is filled in transparent bottles and exposed to sunlight for periods not less than 6 hours (CDC, 2012). The UV irradiation from the sun is able to raise the temperature of the water inactivating microbial contaminants (CDC, 2012; WHO, 2017b). Despite the simplicity of application of SODIS in areas with limited resources, this method of water decontamination is coupled by some limitation. The drawbacks of SODIS is that the volume of water to be treated at a given time is limited, longer time is needed to treat water and large supply of transparent bottles is required (CDC, 2012).

2.5 Photodynamic Antimicrobial Chemotherapy (PACT)

To address some of the problems in water disinfection, there is need to develop other convenient and efficient methods for managing contamination by pathogenic microbial organisms (Jori and Brown, 2004). Photodynamic antimicrobial chemotherapy (PACT) has proven to be a very promising approach for the efficient inactivation of pathogenic microorganisms in water (Carvalho *et al*., 2007). This technique uses the photochemical reaction between three components: a photosensitizer, light of suitable wavelength and molecular oxygen (Hamblin and Jori, 2011). Individually, the three components are not destructive but when in combination toxic ROS are formed. ROS are known to be lethal to cells thus able to destroy pathogenic microbial organisms (Hamblin and Jori, 2011; Straten *et al.*, 2017).

Some of the favorable features of PACT include:

- It can efficiently act on most classes of microbial pathogens including protozoa, fungi and bacteria (Carvalho *et al*., 2007).

- The photodynamic sensitizer can be activated by inexpensive and safe visible light sources (Hamblin and Jori, 2011).
- Antibiotic resistant microbial strain are highly susceptibility to PACT with no selection of photo resistant species reported even after multiple treatments (Tavares *et al.*, 2010).

2.5.1 PACT in Microbial Disinfection

The ability to eradicate microorganisms by PACT was discovered in the beginning of 20th century when Raab observed that the presence of compounds that absorb visible radiation for instance acridine orange and sunlight or artificially produced visible light was able to facilitate the inactivation of unicellular organism *Paramecia* (Raab, 1900). Years later, Jodlbauer and Tappainer (1904) as well showed that oxygen was an essential requirement for photodynamic therapy when they used Photodynamic Therapy (PDT) for the management of skin cancer lesions.

In the subsequent years, research relating to PDT focused in the area of battling cancer and not microbial organisms because the discovery of antibiotics brought about the belief that pathogenic microbial organisms could be progressively reduced to a level that it had no severe effect to humans (Wilson *et al.*, 1995). However, owing to the prompt occurrence of antimicrobial resistant microorganisms, a number of researchers have regained interest in the initial study of Raab in the application of PDT in the elimination of microorganisms (Dobson and Wilson, 1992; Merchat *et al.*, 1996; Okamoto *et al.*, 1990; Wilson *et al.*, 1995). In the year 1990's dental cariogenic bacteria were successfully killed by laser irradiation in the presence of specific dyes (Okamoto *et al.*, 1990). Dobson and Wilson (1992) in their study showed that bacterial species responsible for periodontal diseases can be successfully killed by laser light with an appropriate photosensitizer. A significant step in PACT was in the late 1990's owing to independent discoveries made by three research groups that visible light activatable photosensitizers belonging to the family of phenothiazines (Wilson *et al.*, 1995) and porphyrin (Merchat *et al.*, 1996) were able to induce the killing of both gram positive and negative bacteria. Currently it is known that with the use of a suitable photosensitizer in the presence of a light source various microorganisms can be eliminated (Merchat *et al.*, 1996). Therefore, there is need to synthesize and study the suitability of various photosensitizers for application in PACT.

2.5.2 Mechanism of action of a photosensitizer.

Mechanism of action of photosensitizer begin when the photosensitizer localizes preferentially in the target cell, such as bacterial cell or other high proliferating cells (Wagnières *et al*., 1998). Upon illumination of a photosensitizer with light, Figure 2.3, a photon of light is absorbed (1) promoting the photosensitizer from the ground state (S_0) to the exited singlet state (S_1). In this state, an electron is moved to a higher energy orbital (Wagnières *et al*., 1998), the electron can then return to the singlet ground state (S_0) releasing its energy into heat or fluorescence (2). Alternatively it can change its spin system *via* intersystem crossing (ISC, 3) to give triplet exited state (T_1) that has slightly lower energy than the singlet exited state (Porfirinas and Fotodin, 1996). In the triplet exited state the photosensitizer can transfer its energy by phosphorescence (4) as it returns to ground state. However, because this transition is forbidden the decay of the metastable triplet exited state photosensitizer to the singlet ground state is slow (Porfirinas and Fotodin, 1996), hence it has time to react with molecular oxygen ($^3O_2$) and transfers its energy to produce singlet oxygen ($^1O_2$) (Type II) (5) and free radicals (Type I) (6) which are known to be lethal to cells. Singlet oxygen as well as free radicals are the effective toxic agents in photodynamic mechanisms such as PACT (Moan and Berg, 1992).

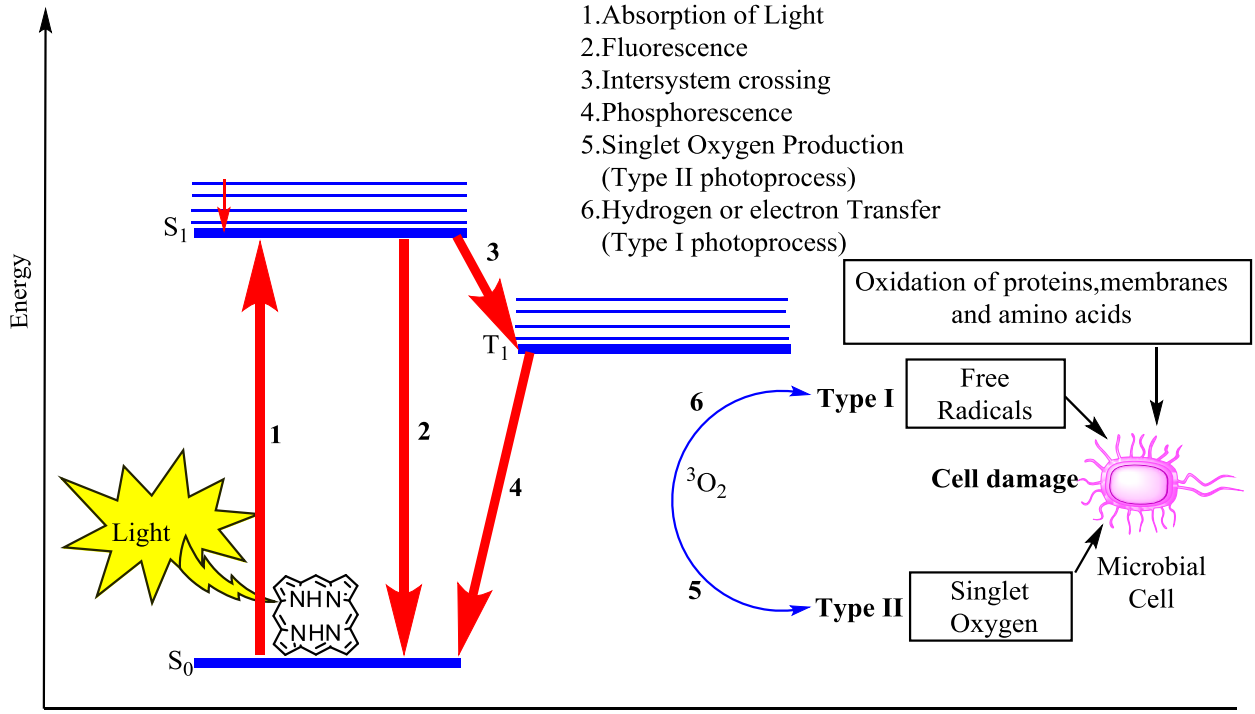

Figure 2.3: Modified Jablonski Diagram for a Typical Photosensitizer (Sternberg *et al.*, 1998).

2.5.2.1 Type I and Type II Photosensitization Reaction

There are two possible mechanisms (Type I and Type II) for the transfer of energy of a photosensitizer both of which require the reactive intermediate to be the long lived photo excited triplet state (T_1).

In Type I mechanism the exited triplet state of the photosensitizer (Sens*) may react directly with the substrate within a cell (e.g. water in cell membrane or the cytoplasm) in a single electron transfer reaction to generate a radical ion in both the photosensitizer and substrate. Electron transfer can occur both ways resulting in formation of substrate radical cation ($Substrate^{\cdot+}$) and a sensitizer radical anion ($Sens^{\cdot-}$) or vice versa. This is then intercepted by ground state molecular oxygen ($^3O_2$) generating a variety of oxidized products leading to loss of photosensitizer as it is converted to an oxidized molecule, Figure 2.4. Alternatively, the extra electron of photosensitizer radical anion ($Sens^{\cdot-}$) can be transferred directly to oxygen to produce cytotoxic ROS (such as superoxide radical anion $O_2^{\cdot-}$) regenerating the original photosensitizer. These highly reactive radicals can quickly pass through cell membranes causing oxidative damage. They can also react in a series of chain reactions with organic substrates (e.g. fatty acids and lipids) to produce more cytotoxic radicals (Foote, 1991).

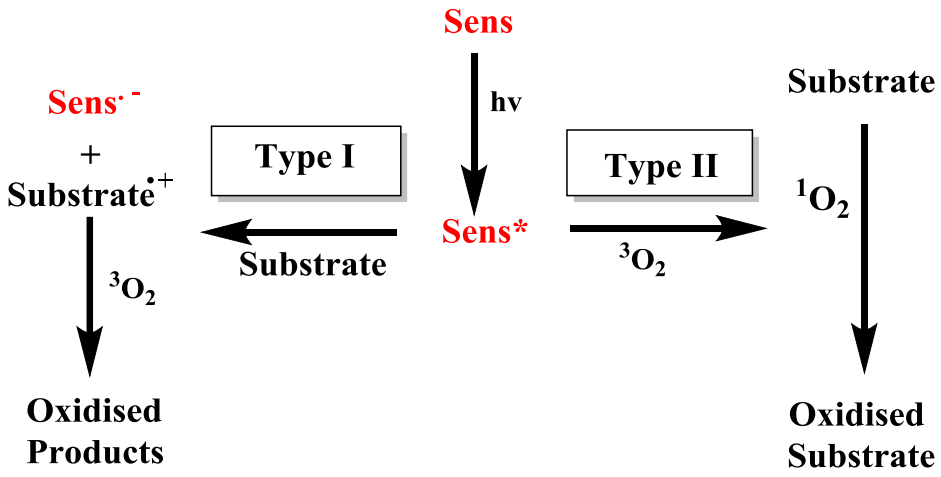

Figure 2.4: Type I vs Type II Photosensitization Reaction

Type II mechanism pathway occurs when the excitation energy from triplet state photosensitizer (Sens*) is transferred to molecular oxygen ($^3O_2$) in its ground state (triplet) found in most cells to

produce highly reactive (toxic) singlet oxygen ($^1O_2$). $^1O_2$ is a powerful oxidant that reacts with biological components within the cell such as DNA bases and proteins leading to cell death. In the process the exited photosensitizer regenerates to ground state photosensitizer (Porfirinas and Fotodin, 1996).

2.6 Photosensitizers

Photosensitizers are compounds which allow the transfer and transformation of light energy into type I and II chemical reactions producing reactive toxic end product that can damage cell structures leading to cell death (Deda and Araki, 2015). An ideal photosensitizer for PACT is one which is safe, able to absorb photons efficiently at longer wavelength (preferable visible region 400-700nm), has a high probability of triplet state formation and the triplet state should be long lived to have time to react with other molecules in the environment (Allison *et al*., 2004; Deda and Araki, 2015). Photosensitizers can be categorized based on their chemical structure or generation gap (Allison *et al*., 2004).

They can be classified into three major families based on their chemical structure: porphyrin family, chlorophyll family and dyes (Allison *et al*., 2004). Porphyrin family are those photosensitizers with a porphyrin platform, they include Hematoporphyrin and its derivatives, Benzoporphyrin derivatives and Texaphyrins. Chlorophyll family consists of photosensitizers with a chlorophyll platform, they include chlorins and bacteriochlorins. The Dyes Phthalocyanine and Naphthalocyanine have potential application as photosensitizes in PDT (Allison *et al*., 2004). Table 2.1 below shows classification of photosensitizers in three families based on their chemical structure.

Table 2.1: Classification according to photosensitizer families (Allison *et al*., 2004).

PORPHYRIN FAMILY	**CHLOROPHYLL FAMILY**	**DYES**
Hematoporphyrin and derivatives	Chlorins	Phthalocyanine
Benzoporphyrin	Bacteriochlorins.	Naphthalocyanine

Based on generational gap they can be grouped as first generation, second generation and third generation photosensitizers. First generation are those developed in the 1970s and early 1980s

which are basically naturally occurring porphyrins and their derivatives (Allison *et al*., 2004). Second generation refers to those which came to existence from late 1980s onwards aimed at solving limitations present in the first generation photosensitizers. They include chlorin, bacteriochlorin and dyes. These photosensitizers have a characteristic long wavelength of absorption and low toxic side effects while third generation contains first and second generation photosensitizers conjugated with biomolecules, nanoparticles etc. with the intention of improving activity of the photosensitizer by increasing its selectivity and bioavailability (Allison *et al*., 2004; Deda and Araki, 2015). Figure 2.5 below shows chemical structures of some common photosensitizers.

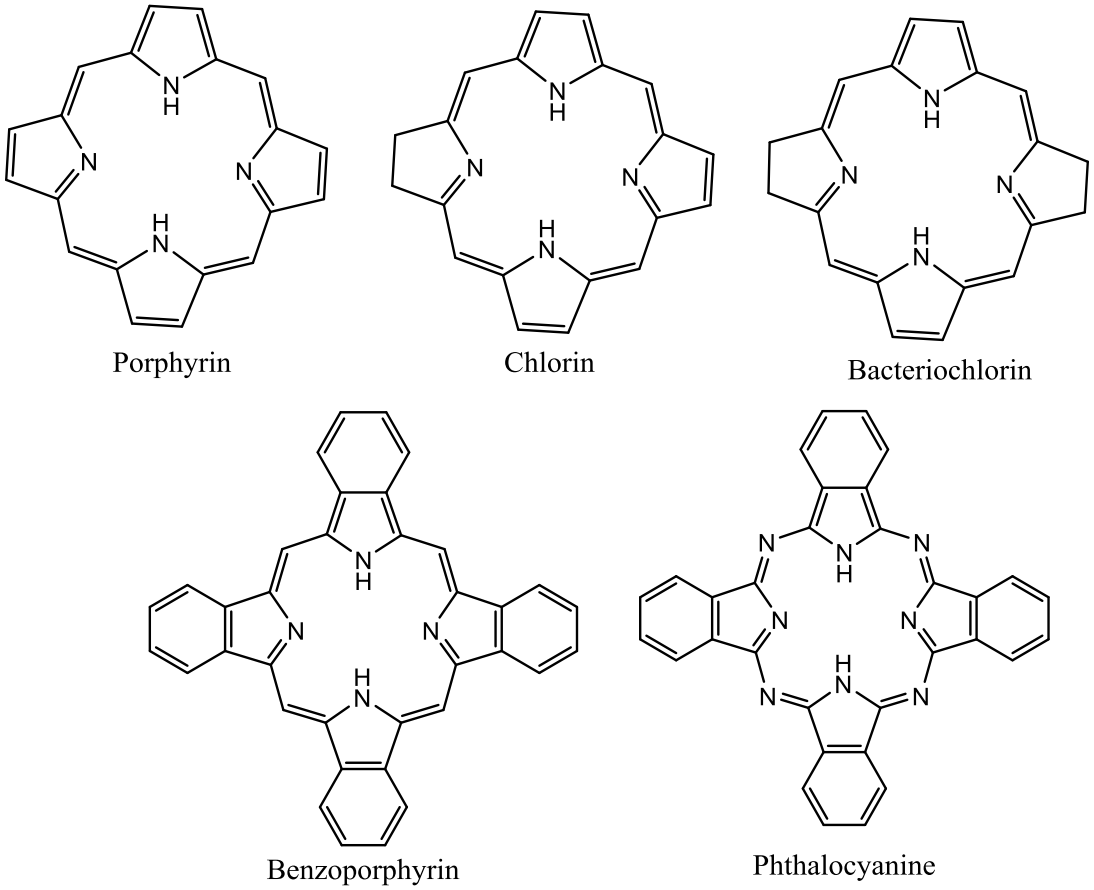

Figure 2.5: Chemical structures of some common photosensitizers (Deda and Araki, 2015).

2.7 Porphyrin

"Porphyrin" is a word originating from the Greek work *porphura* meaning purple (Rastogi and Dwivedi, 2006). They are aromatic organic compounds which could be either of natural or

synthetic in origin. Naturally occurring porphyrin perform a variety of important functions in nature. They are found as constituents of essential components in both plants and human body. They are constituents of chlorophyll in which the core is chelated with magnesium; coenzyme B12 with the core chelated nickel and heme proteins chelated with iron (Rastogi and Dwivedi, 2006).

Porphyrin is a highly conjugated molecule having 22π electrons. They are vastly colored with the structure having four pyrrole units linked through methine (–CH=) bridges to form a porphyrin macrocycle, Figure 2.6.

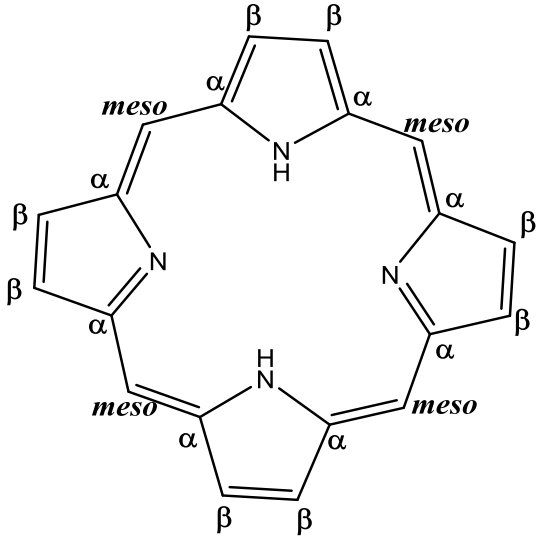

Figure 2.6: Chemical structure of a porphyrin showing α, β and *meso* position (Rastogi and Dwivedi, 2006).

The intense color of porphyrin is said to be due to the presence of double bonds linking the pyrrole units (Rastogi and Dwivedi, 2006). Porphyrins have key biological and photophysical properties that attract the interest of various researchers (Cavaleiro and Smith, 1987). They are highly stable, absorb within the visible region of the spectrum, non-toxic in the dark and are fluorescent (Rastogi and Dwivedi, 2006). The nitrogens of the pyrrole subunit in the porphyrin macrocycle can act as a free base able to form a variety of stable complexes with metals forming metalloporphyrin (Vicente, 2001). There are 12 positions that can be substituted at porphyrin molecule, 8 at the pyrrole sub units (β-position) and 4 at the methine bridges (*meso* position) (Arnaut, 2011; Rastogi and Dwivedi, 2006).

Although there are more β positions available in porphyrin macrocycle to be substituted, *meso*-substituted porphyrin has been extensively investigated compared to β-substituted porphyrin. This is because, compared to β-substituted porphyrins *meso*-substituted porphyrins are relatively easy to synthesize (Amuhaya, 2011). Additionally, highly sophisticated and reactive functional groups can be easily designed at the *meso* position (Amuhaya, 2011).

2.7.1 Absorption Spectra of Porphyrins

Porphyrins have a characteristic UV-VIS spectrum appearing near UV and Visible region of the electromagnetic spectrum, Figure 2.7.

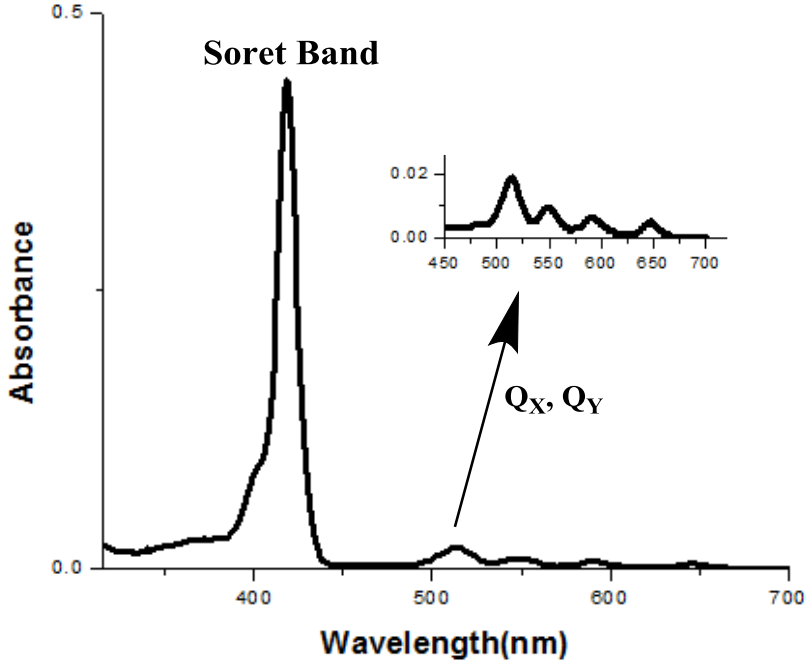

Figure 2.7: Diagram showing UV-VIS absorption spectrum for porphyrin molecule (Shekar, 2013).

Their spectrum is characterized by an intense band called the soret or B band at about 400nm (blue region) and four weak Q bands observed between 500-600nm (red region). Metallation of porphyrin macrocycle has effect on its absorption spectrum. The UV-Vis spectrum retains the B band (soret) absorption spectrum while the four Q band is simplified to two upon metallation (Shekar, 2013). The simplification of UV-Vis spectrum is attributed to the change in symmetry of porphyrin macrocycle due to metallation (Huang *et al*., 2000).

2.7.2 Gouterman four-orbital model

In an attempt to provide an explanation for the absorption spectra displayed by porphyrin, Gouterman suggested the four-orbital model (Gouterman, 1961). According to this model, the Soret and Q absorption bands of porphyrins both arise from the $\pi \rightarrow \pi^*$ transition between two non-degenerate HOMOs and two degenerate LUMOs**.** Transitions between these two HOMOs and two LUMOs gives rise to two exited singlet states, Figure 2.8**.**

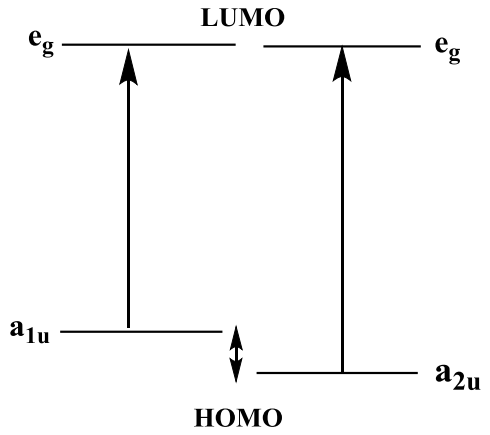

Figure 2.8: Gouterman four orbital model for possible porphyrin transitions (Gouterman, 1961).

Orbital mixing splits the two exited singlet states in energy generating a high energy S_2 state and a lower energy S_1 state. Transition to the high energy state, S_2 state, is the origin of the soret band while transition to the low energy state, S_1 state, brings about the less intense Q bands, Figure 2.9. The corresponding energy of transition depends on the substituents on the porphyrin ring and the central metal's electronic nature (Gouterman, 1961; Gouterman *et al.*, 1963; Weaver, 2005).

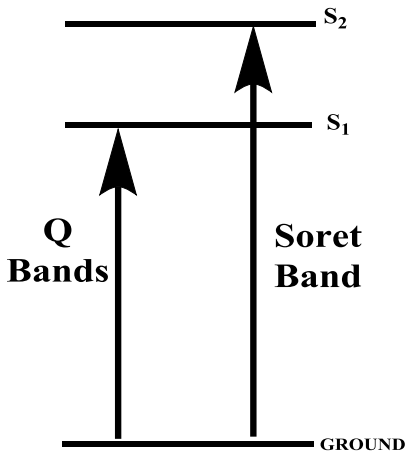

Figure 2.9: State Diagram showing possible exited states of porphyrin (Weaver, 2005)

2.8 Synthesis of Porphyrins

Porphyrin synthesis has attracted attention due to the important roles it plays in photosynthesis, oxygen transport, biological reaction and material science (Gouterman, 1961; Lindsey *et al*., 1987). Porphyrins can be synthesized from scratch in the laboratory or acquired directly from nature. Nature provides a wide variety of porphyrins like chlorophyll from which other derivatives can be made. However, porphyrins acquired from nature are mostly β-substituted. In order to develop porphyrins with diverse patterns of substitution, there is need to begin synthesis of the target porphyrin from scratch (Sekhar, 2013). There are several methods that have been developed over the years for the synthesis of *meso*-substituted porphyrins. Some of the developed and commonly used protocols are discussed below.

2.8.1 Rothemund Method

Rothemund in 1940s pioneered the synthesis of *meso*-tetraphenyl porphyrin (TPP) (Rothemund and Menotti, 1941). *Meso*-TPP was synthesized by condensing pyrrole and benzaldehyde in pyridine solution in a closed tube at 220˚C for forty-eight hours (Rothemund and Menotti, 1941), Scheme 2.1. In addition, Rothemund also observed that *meso*-TPP was synthesized when pyrrole, benzaldehyde and pyridine were refluxed in a methanol solution for a number of days at atmospheric pressure (Rothemund and Menotti, 1941).

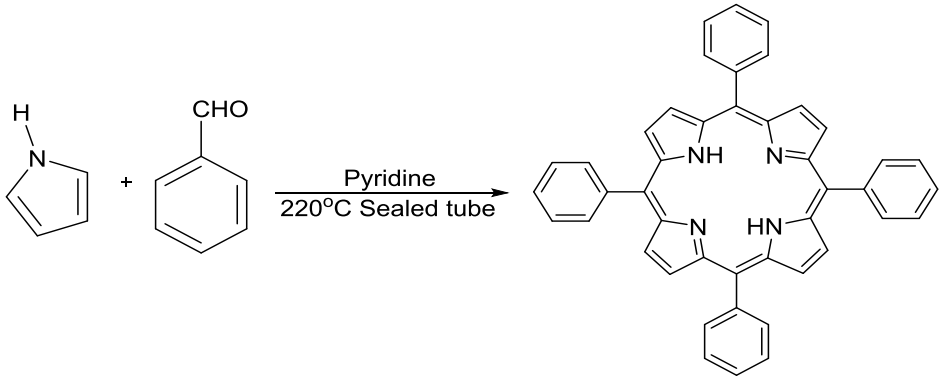

Scheme 2.1: Rothemund method of porphyrin synthesis (Rothemund and Menotti, 1941).

Although the Rothemund method was a success in the synthesis of *meso*-TPP, the yield from the synthesis was low and the reaction condition so rigorous that only a small number of substituted aldehydes could be transformed to the corresponding porphyrin (Lindsey *et al.*, 1987).

2.8.2 Adler-Longo Method

In the 1960s, Adler and Longo adjusted the Rothemund method to improve on the synthesis of TPP (Adler *et al.*, 1967). In open air, freshly distilled pyrrole and reagent grade benzaldehyde were allowed to react in refluxing propionic acid (141°C) for 30 minutes, cooled to room temperature conditions and filtered (Lindsey, 1994), Scheme 2.2. The yield and rate of reaction was shown to be determined by initial concentration of reagents, temperature, availability of atmospheric oxygen and acidity (Adler *et al.*, 1967).

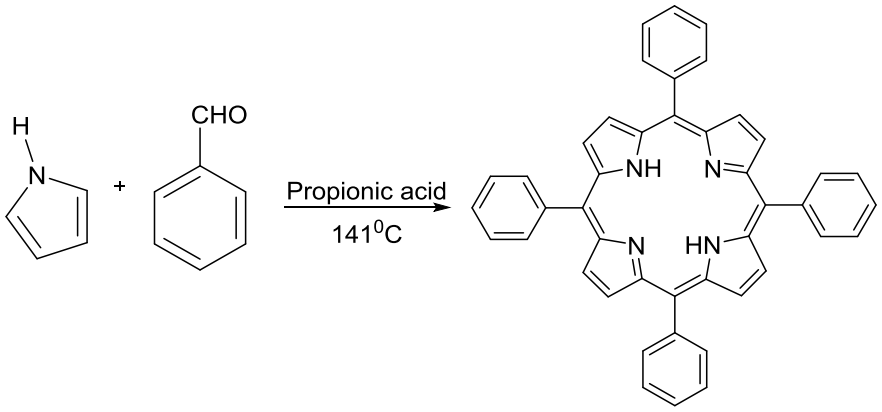

Scheme 2.2: Adler-Longo method of porphyrin synthesis (Adler *et al.*, 1967)

The Adler-Longo method presents a relatively milder condition for the synthesis of several other *meso*-substituted porphyrins by allowing a wider selection of substituted benzaldehyde to be used with yields of upto 20% (Adler *et al.*, 1967). Additionally, the reaction can be carried out at relatively higher concentration and porphyrin is synthesized in crystalline form without the need for further chromatography (Adler *et al*., 1967; Lindsey, 1994).

On the other hand, the method is affected by some problems. First the reaction condition sometimes results in total failure especially when using aldehydes having sensitive functional groups (Lindsey *et al.*, 1987). Second, there is increased solubility of the synthesized porphyrin due to the formation of porphyrin acid salts (Lindsey *et al.*, 1987). Increased solubility and high level of tar produced using this method provides a challenge in the purification of the synthesized porphyrins (Adler *et al.*, 1967; Lindsey *et al.*, 1987).

2.8.3 Lindsey Method

In 1987, Lindsey revisited the Rothemund and Alder-Longo reactions for the synthesis of tetraphenylporphyrins (TPP) and developed a two-step synthesis of porphyrins (Lindsey *et al.*, 1987). Cyclic tetraphenyl porphyriongen was formed by reacting pyrrole and the preferred benzaldehyde in an acid catalyst at room temperature, Scheme 2.3. Oxidative dehydrogenation was then achieved using a suitable oxidant like 2,3-Dichloro-5,6-dicyano-1,4-benzoquinone (DDQ) or p-chloranil to form a stable porphyrin molecule. Lindsey's protocol provides a suitable alternative for the synthesis of porphyrins when using aldehydes bearing sensitive functional groups with minimum difficulty in purification. The final yield of porphyrin synthesized was mainly determined by concentration of benzaldehyde and pyrrole. Maximum yield (30%) was observed at equimolar benzaldehyde and pyrrole concentration of 10^{-2} M (Lindsey *et al.*, 1994; Lindsey *et al.*, 1987).

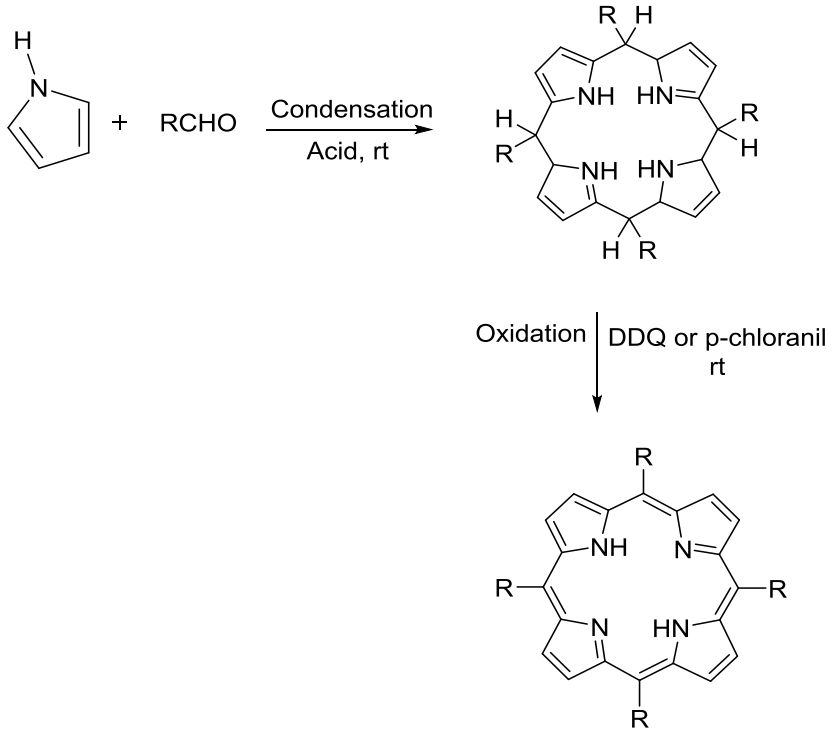

Scheme 2.3: Lindsey's two-step synthesis of Porphyrin (Lindsey, 2010).

2.8.4 Porphyrins from Dipyrromethane

Dipyrromethane consist of two pyrrole units linked through methine bridges. In the presence of aldehyde, acid catalyst and an oxidant, two dipyrromethane units can be merged to synthesize various target porphyrin compounds through a process referred to as [2+2] condensation (Lindsey,

2010). This protocol provides a suitable alternative for the synthesis of *trans* substituted porphyrins with insignificant concentration of isomeric porphyrins being detected in the reaction solution (Amuhaya, 2011; Lindsey, 2010). The dipyrromethane units can be successfully synthesized using a variety of established methods, however, the one flask synthesis is the most preferred due to convenience and scalability. It involves the condensation of pyrrole and desired benzaldehyde at room temperature conditions in an acid (TFA or $BF_3.O(Et)_2$ or $InCl_3$). Pyrrole acts as a solvent during synthesis with a high pyrrole to aldehyde ratio of (25:1 to 100:1). The high pyrrole to aldehyde ratio suppresses oligomerization beyond dipyrromethane stage (Lindsey, 2010).

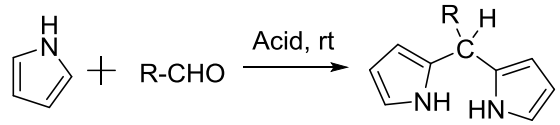

Scheme 2.4: Synthesis of Dipyrromethane (Amuhaya, 2011)**.**

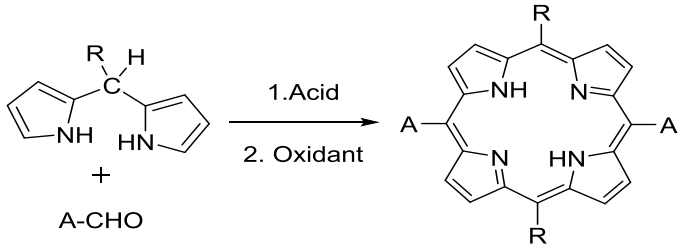

Scheme 2.5: [2+2] condensation for *trans*-A_2B_2-porphyrin synthesis (Amuhaya, 2011).

Despite the success of [2+2] condensation method in the rational synthesis of *trans* substituted porphyrins, the method is often burdened with scrambling process. The process is initiated with the acid protonation of the α position of pyrrole in pyrromethane or porphyrinogen species. This is followed by shifting of the neighboring pyrrole units and finally unsolicited recombination of the subsequent fragments (Chevalier *et al.*, 2002; Lindsey, 2010), Scheme 2.6.

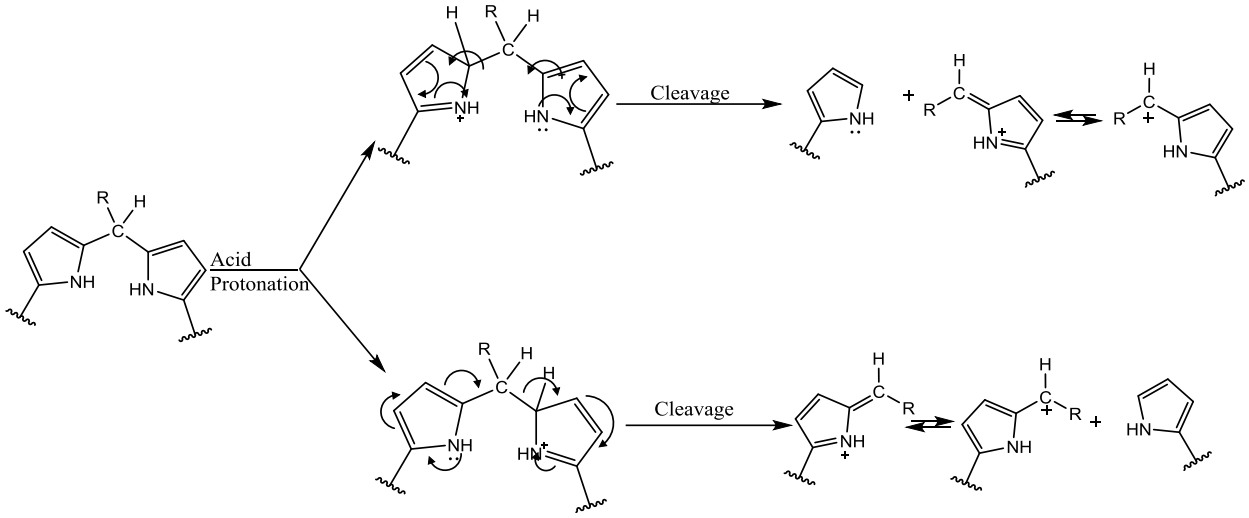

Scheme 2.6: Scrambling during porphyrin synthesis (Chevalier *et al.*, 2002)

This results to forming a completely different compound, formation of a mixture of porphyrins, synthesis of the target compound in very low yield as well as practical difficulty in separating the synthesized compounds. The success of this method involves optimizing the reaction condition to minimize scrambling thus resulting to rational synthesis of the target porphyrin (Amuhaya, 2011; Chevalier *et al.*, 2002; Lindsey, 2010).

For this work the Adler-Longo method (Adler *et al.*, 1967) was used for the synthesis of freebase 5,10,15,20-tetra(4-bromophenyl)porphyrin, (H_2TBrPP**)**, while freebase 5,10,15,20-tetra(pyren-1-yl)porphyrin, (H_2TPyP), was synthesized using the Lindsey method. This was after failure of the Adler-Longo method to yield viable results for the synthesis of freebase H_2TPyP as most of the pyrene-1-carbaldehyde starting material would remain unreacted at the end of the reaction.

CHAPTER THREE
MATERIALS AND METHODS

3.1 Materials

All chemicals and organic solvents used in this study were of analytical grade and used without further purification. Pyrrole was freshly distilled prior to use. Solvents were dried using molecular sieves obtained from Sigma-Aldrich and were pre-dried at 250 ℃ for 24 hours immediately before use. Sample purification was done using Merck silica gel 60 (70 – 230 mesh) and reaction progress monitored through thin layer chromatography using silica gel 60 (F_{254} Merck) plates. The UV-Vis absorption measurements were recorded on a Shimadzu UV Spectrophotometer UV-1800 with a spectral range of 200 – 800 nm. The carbon, hydrogen and nitrogen (CHN) content of the synthesized compounds were determined by Vario-Elementar Microcube ELIII. Mass spectral data was recorded in a Bruker AutoFLEX III Smartbeam TOF/TOF Mass spectrometer. The instrument was operated on positive ion mode and spectrum was acquired using dithranol as the MALDI matrix. ^{1}H NMR spectra was recorded using a Bruker AVANCE 600MHz NMR spectrometer using Tetramethyl silane (TMS) the spectra processed using MestReNova 10.0 software. The spectrum of the freebase H_2TPyP and its corresponding metal conjugates Zn(II), Ga(III) were recorded in deuterated chloroform while that for the In(III) conjugate was recorded in deuterated DMSO-d_6. Fluorescence measurements were recorded on a Shimadzu RF-6000 Spectrofluorophotometer.

3.2 Synthetic Procedures

3.2.1 Synthesis of 5,10,15,20-tetra(4-bromophenyl) porphyrin (H_2TBrPP)

H_2TBrPP was prepared using the Adler-Longo method (Adler *et al.,* 1967) whereby to a refluxing solution of propionic acid (25 mL), 4-bromobenzaldehyde (0.50 g, 2.7 mmol) and freshly distilled pyrrole (0.19 mL, 2.7 mmol) was added. The reaction mixture was refluxed for 3 hours. After completion of the reaction, contents of the flask was left to cool overnight to give a solid residue which was filtered off and washed with methanol to give a purple solid. The crude product was purified in a silica gel column using solvent system ethyl acetate/hexane (1:4) to obtain the target product as a purple solid, yield 47% (0.29 g).

3.2.2 Synthesis of 5,10,15,20-tetra(pyren-1-yl)porphyrin (H_2TPyP)

H_2TPyP was prepared using modification of the Lindsey protocol (Lindsey, 2010). Pyrene-1-

carbaldehyde (0.50 g, 2.17 mmol) was dissolved in dry DCM. The flask was purged with nitrogen before freshly distilled pyrrole (0.15 mL, 2.16 mmol) was added. TFA was injected and stirred at room temperature for 1.5 hours. DDQ was added and the reaction stirred for 1 hour at room temperature. It was then neutralized with TEA. The crude product was purified in a silica gel column using solvent system ethyl acetate/hexane (1:5) to obtain the target product as a purple solid, yield 23% (0.14 g).

3.2.3 Synthesis of Zn 5,10,15,20-tetra(pyren-1-yl)porphyrin (ZnTPyP)

ZnTPyP was prepared by dissolving (0.08 g, 0.072 mmol) of 5,10,15,20-tetra(pyren-1-yl)porphyrin in DCM/MeOH (3:1) and adding zinc acetate (0.04 g, 0.216 mmol). The reaction mixture was stirred at room temperature for 48 hours, contents of the flask was then washed with water and dried in a vacuum. The crude product was purified in a silica gel column using DCM as the eluent to obtain the target porphyrin compound, yield 93% (0.08 g).

3.2.4 Synthesis of Gallium Chloride 5,10,15,20-tetra(pyren-1-yl)porphyrin (GaClTPyP)

The target compound GaClTPyP was prepared by the metalation of H_2TPyP as follows: (0.05 g, 0.045 mmol) of 5,10,15,20-tetra(pyren-1-yl)porphyrin was dissolved in 30 mL toluene. $GaCl_3$ (0.20 g, 1.14 mmol), anhydrous K_2CO_3 (0.30 g, 2.39 mmol) and sodium acetate (0.06 g, 0.72 mmol) was added and allowed to reflux under nitrogen for 48 hours. Contents of the flask was neutralized with acetic acid and washed with water. The solvent was removed *in vacuo* and the crude product was purified in a silica gel column using DCM as eluent to obtain the target compound, yield 81% (0.04 g).

3.2.5 Synthesis of Indium Chloride 5,10,15,20-tetra (pyren-1-yl)porphyrin (InClTPyP)

The target compound InClTPyP was prepared according to the reported literature method for indium (III) complex of tetraphenylporphyrin (Batti and Mast, 1972), which was adopted as follows: (0.13 g, 0.117 mmol) of the free base 5,10,15,20-tetra(pyren-1-yl)porphyrin was dissolved in 40 mL acetic acid. Sodium acetate (0.15 g, 1.83 mmol) and indium (III) chloride (0.07 g, 0.32 mmol) were added and resulting mixture refluxed for 36 hours. Contents of the flask was cooled to room temperature, mixed with water and then the product extracted into DCM. Crude product was purified by passing through a silica gel column using DCM as eluent to obtain the target compound, yield 87% (0.12 g).

3.3 Physical and Spectroscopic data of the synthesized compounds

3.3.1 H_2TBrPP

Purple powder; UV-Vis (λ_{max} nm) (DMF): 420, 515, 550, 585, 650; MALDI-TOF- MS (*m/z*): Calc. 929.890, Found 931.885 $[M+2H]^{2+}$; Calc. for H_2TBrPP $C_{44}H_{26}Br_4N_4$ (%): C (56.81), H (2.82), N (6.02), Found: C (56.53), H (2.69), N (5.74); ^{1}H NMR (600 MHz, Chloroform-*d*) δ 8.99 (*s*, 8H), 8.07 – 8.04 (*d*, *J* = 8.0 Hz, 8H), 7.80 – 7.63 (*d*, *J* = 8.0 Hz, 8H), -2.64 (*s*, 2H).

3.3.2 H_2TPyP

Purple powder; UV-Vis (λ_{max} nm) (DMF): 431, 520, 555, 595, 655; MALDI-TOF- MS (*m/z*): Calc. 1110.370, Found 1111.302 $[M+H]^+$; Calc. for H_2TPyP $C_{84}H_{46}N_4$ (%): C (90.79), H (4.17), N (5.09), Found C (90.38), H (4.13), N (4.98); ^{1}H NMR (600 MHz, Chloroform-*d*) δ 8.91 – 8.77 (*m*, 4H), 8.60 – 8.50 (*m*, 4H), 8.48 – 8.43 (*m*, 12H), 8.43 – 8.30 (*m*, 12H), 8.17 – 8.04 (*m*, 4H), 7.78 – 7.70 (*m*, 4H), 7.55 – 7.45 (*m*, 4H), -2.40 (*s*, 2H).

3.3.3 ZnTPyP

Purple powder; UV-Vis (λ_{max} nm) (DMF): 439, 562, 603; MALDI-TOF-MS (*m/z*): Calc. 1172.290, Found 1173.673 $[M+H]^+$; Calc. for ZnTPyP $C_{84}H_{44}N_4Zn$ (%): C (85.89), H (3.78), N (4.77), Found: C (85.62), H (3.81), N (4.53); ^{1}H NMR (600 MHz, Chloroform-*d*) δ 8.92 – 8.75 (*m*, 4H), 8.65 – 8.57 (*m*, 4H), 8.50 – 8.42 (*m*, 12H), 8.40 – 8.27 (*m*,12H), 8.17 – 8.02 (*m*, 4H), 7.81 – 7.75 (*m*, 4H), 7.63 – 7.48 (*m*, 4H).

3.3.4 GaClTPyP

Purple powder; UV-Vis (λ_{max} nm) (DMF): 440, 563, 605; MALDI-TOF-MS (*m/z*): Calc. 1212.250, Found 1178.510 $[M+H-Cl]^+$, 1109.574 $[M+H-(Cl+Ga)]^+$; Calc. for GaClTPyP $C_{84}H_{44}ClGaN_4$ (%): C (83.07), H (3.65), N (4.41), Found: C (83.14), H (3.48), N (4.29); ^{1}H NMR (600 MHz, Chloroform-*d*) δ 8.92 – 8.78 (*m*, 4H), 8.51 – 8.45 (*m*, 4H), 8.41 – 8.38 (*m*,12H), 8.38 – 8.33 (*m*, 12H), 8.15 – 8.02 (*m*, 4H), 7.82 – 7.75 (*m*, 4H), 7.63 – 7.55 (*m*, 4H).

3.3.5 InClTPyP

Purple powder; UV-Vis (λ_{max} nm) (DMF): 443, 571, 611; MALDI-TOF-MS (*m/z*): Calc. 1258.230, Found 1259.418 $[M+H]^+$, 1224.440 $[M+H-Cl]^+$; Calc. for InClTPyP $C_{84}H_{44}ClInN_4$(%): C (80.10), H (3.52), N (4.45), Found: C (79.98), H (3.47), N (4.39). ^{1}H NMR (600 MHz, DMSO-d_6) δ 8.96 – 8.81 (*m*, 4H), 8.77 – 8.63 (*m*, 4H), 8.53 – 8.49

(*m*, 12H), 8.44 – 8.40 (*m*, 12H), 8.34 – 8.22 (*m*,4H), 8.2 – 8.12 (*m*, 4H), 7.88 and 7.46 (*m*, 4H).

3.4 Photophysical Studies

3.4.1 UV-Vis spectroscopy

The UV-Vis absorption measurements were recorded on a Shimadzu UV Spectrophotometer UV-1800 with a spectral range of 200 – 800 nm. All experiments were carried out at room temperature in DMF using a pair of 10 mm quartz cell cuvettes. The spectrometer was calibrated using a blank before scanning the sample in 1 µM concentration and recording their spectra.

3.4.2 Fluorescence Spectroscopy

Fluorescence measurements was done at room temperature conditions by preparing solutions of the standard and sample in DMF. The absorbance of each was determined in UV-Vis and concentrations with absorbance below 0.1 were chosen to reduce inner filter effect. The fluorescence emission spectra of these samples were recorded on a Shimadzu RF-6000 Spectrofluorophotometer with an excitation of 411 nm using a pair of 10 mm quartz cell cuvettes. A fluorescence instrument sends light through a sample, excites the electron and then reads the radiation released when electrons returns to ground state. The area under emission spectra were calculated and fluorescence quantum yield (ϕ_F) determined by comparative method (Fery-Forgues and Lavabre, 2009) according to Equation 1.

$$\phi_F = \phi_F^{Std} \frac{FA^{Std}n^2}{F^{Std}A(n^{Std})^2} \qquad \text{Equation 1.}$$

Where F and F^{Std} are the areas under the fluorescence emission curves of the porphyrin and standard, respectively. A and A^{Std} are the optical absorbance of the sample and standard respectively at the excitation wavelength. n and n^{Std} are the refractive indices of the solvent used to dissolve the sample and the standard respectively. ϕ_F^{Std} is the fluorescence quantum yield for the standard. TPP (ϕ_F = 0.11) (Silva *et al.,* 2012) was used as the standard for the free base porphyrin and ZnTPP (ϕ_F = 0.033) (Brookfield *et al.,* 1985) was used as the standard for metallated porphyrins.

3.5 Antimicrobial Studies

PACT properties of the synthesized porphyrin derivatives H_2TBrPP, H_2TPyP, ZnTPyP and InClTPyP against Gram-positive bacteria *Staphylococcus aureus* were evaluated by measuring the % cell viability at different photosensitizer concentration. *S. aureus* (ATCC 6538) was purchased from Microbiologics. Photo-irradiations for antimicrobial studies were performed using a General Electric Quartz lamp (300W). Photoinactivation studies were carried out according to literature method (Osifeko *et al.*, 2016; Mantareva *et al.*, 2007). Briefly, stock solution of the photosensitizers was prepared by dissolving a known amount of the photosensitizer in 5% DMSO. The stock solution was then diluted to concentrations of 40, 35, 30, 25, 20, 15, 10 and 5 µg/mL. *Staphylococcus aureus* bacteria was grown on a nutrient agar plate prepared according to the 3 .manufactures specification to obtain colonies. A single colony of *S. aureus* from the agar plate was aseptically transferred to 10ml nutrient broth and allowed to grow at 37° until an optical density of approximately 0.6 – 0.8 at 600 nm was obtained. The bacteria were harvested through removal of broth by centrifugation (3000 rpm for 15 min), washed once with Phosphate buffer saline (PBS, pH 7.4) and re-suspended in 4 mL PBS.

In the dark and at room temperature, 100 µL solutions of the samples (H_2TBrPP, H_2TPyP, ZnTPyP and InClTPyP) at different concentration of 40, 35, 30, 25, 20, 15, 10 and 5 µg/mL were independently added to 96-well plates containing 100 µL of the bacteria culture aliquots of *S. aureus* prepared in the first step. The plates were then irradiated with light at a fluence rate of 0.05 W cm^{-2} for 15 minutes. Dark toxicity was determined under the same condition but without irradiation with light. Two controls were included; PBS and the bacteria with no photosensitizers added. The controls provided data on the cell's response to light exposure in the absence of a photosensitizer. The irradiated and non-irradiated plates were then incubated in the dark at 37° in an incubator shaker at approximately 200 rpm. All the experiments were conducted in triplicate. The optical density of the bacteria in each plate was determined at 600 nm after 24 hours and % cell viability at different photosensitizer concentration was calculated as:

$$\%\ \text{Cell Viability} = \frac{OD_T}{OD_C} \times 100 \qquad \text{Equation 2}$$

Where OD_T and OD_C are the optical density of the treated and control cells respectively.

CHAPTER FOUR
RESULTS AND DISCUSSION

Outline of the study

In this study 5,10,15,20-tetrakis(4-bromophenyl)porphyrin (H_2TBrPP), 5,10,15,20-tetra(pyren-1-yl)porphyrin (H_2TPyP), zinc 5,10,15,20-tetra(pyren-1-yl)porphyrin (ZnTPyP), gallium chloride 5,10,15,20-tetra(pyren-1-yl)porphyrin (GaClTPyP) and indium chloride 5,10,15,20-tetra (pyren-1-yl)porphyrin (InClTPyP) were synthesized and purified using column chromatography. The compounds were characterized using mass spectrometry, elemental analysis and ^{1}H NMR spectroscopy. To determine the suitability of the compounds for PACT their photophysical properties were determined using UV-Vis and fluorescence spectroscopy. PACT studies were done against *Staphylococcus aureus* bacteria.

4.1 Synthesis and Characterization of porphyrin derivatives

4.1.1 H_2TBrPP

The Adler-Longo method (Adler *et al.*, 1967) was used for the synthesis of freebase H_2TBrPP using 4-bromobenzaldehyde and pyrrole in 47% yield, Scheme 4.1.

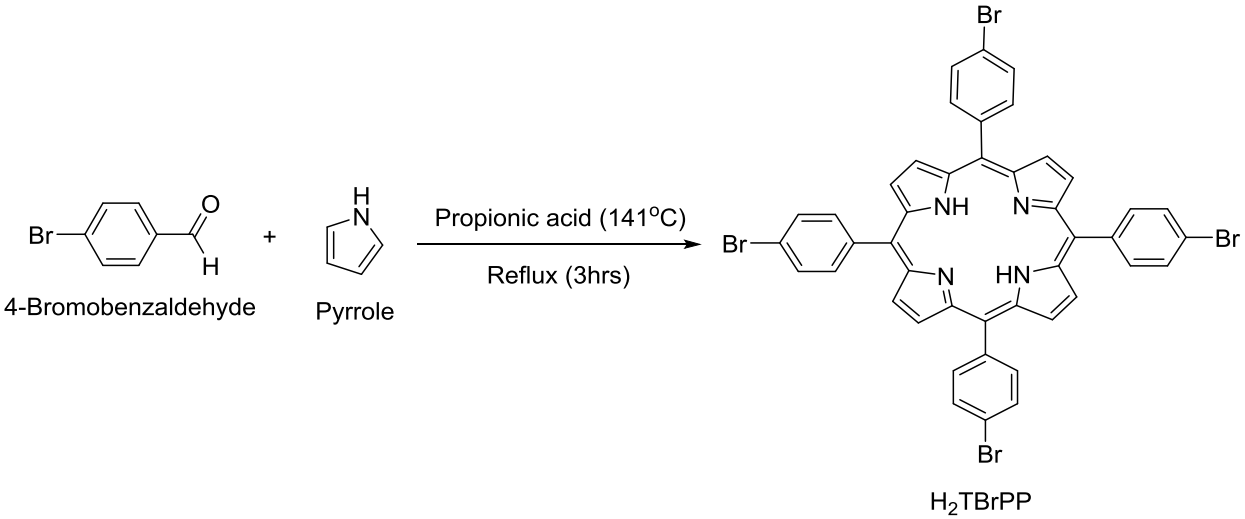

Scheme 4.1: Synthesis of H_2TBrPP

The UV-Vis spectrum of H_2TBrPP showed soret band at 420 nm while the Q bands were observed at 515, 550, 585 and 650 nm which is typical of porphyrin derivatives (Gouterman, 1961). Studies carried out by Gouterman (Gouterman, 1961) attributed this to $\pi \rightarrow \pi^*$ transition between two HOMOs and two LUMOs, See Section 2.7.2. Transition between these two HOMOs and two

LUMOs brings about two exited states. Out of the two exited states, a high energy state S_2 and low energy state S_1 is established as a result of orbital mixing splitting the energy of exited states (Gouterman, 1961). Transition to the high energy state effected the observed soret band while transition to the low energy state brought forth the observed less intense Q bands (Gouterman, 1961). The mass spectral data obtained for the compound displayed a molecular ion peak at 931.885 $[M+2H]^{2+}$, calculated 929.89, Appendix A.1, for $C_{44}H_{26}Br_4N_4$. The elemental analysis data (%) showed that the CHN composition of H_2TBrPP was: C (56.53), H (2.69), N (5.74) and calculation of composition of CHN from this data as shown below is in agreement with the molecular formula of this compound.

Experimental CHN composition C 55.53, H 2.69, N 5.74

C $\frac{56.53}{100} \times 929.89 = 525.67$ H $\frac{2.69}{100} \times 929.89 = 25.81$ N $\frac{5.74}{100} \times 929.89 = 53.38$

12.01 amu = 1 Carbon 1.00 amu = 1 Hydrogen 14.01 amu = 1 Nitrogen

525.67 = ? 25.81 = ? 53.38 = ?

C $\frac{525.67}{12.01} \times 1 = 43.77 \approx 44$ H $\frac{25.81}{1} \times 1 = 25.81 \approx 26$ N $\frac{53.38}{14} \times 1 = 3.8 \approx 4$

The ^{1}H NMR spectrum showed a singlet at δ_H -2.64 (*s*, 2H) which was assigned to the highly shielded protons on the nitrogen bound pyrrole protons (Bajju *et al*., 2013), Appendix A.2. This is due to the large π conjugation in the porphyrin macrocycle which enhances the "aromatic ring current" effect, thus producing a shielding effect on protons inside the macrocycle and deshielding effect on protons outside (Falvo *et al.,* 1999; Peeks *et al*., 2017). The aromatic β-pyrrole protons resonated as a singlet at δ_H 8.99 and the *meso*-aryl protons resonated as a doublet at δ_H 8.05 and δ_H 7.78 (*J* = 8.0 Hz, 8H) for the sixteen aromatic protons of the four bromophenyl *meso* substituents.

4.1.2 H_2TPyP

The Lindsey protocol (Lindsey, 2010) was adopted for the synthesis of the freebase H_2TPyP porphyrin using pyrene-1-carbaldehyde as the aldehyde and pyrrole with yield of 23%, Scheme 4.2.

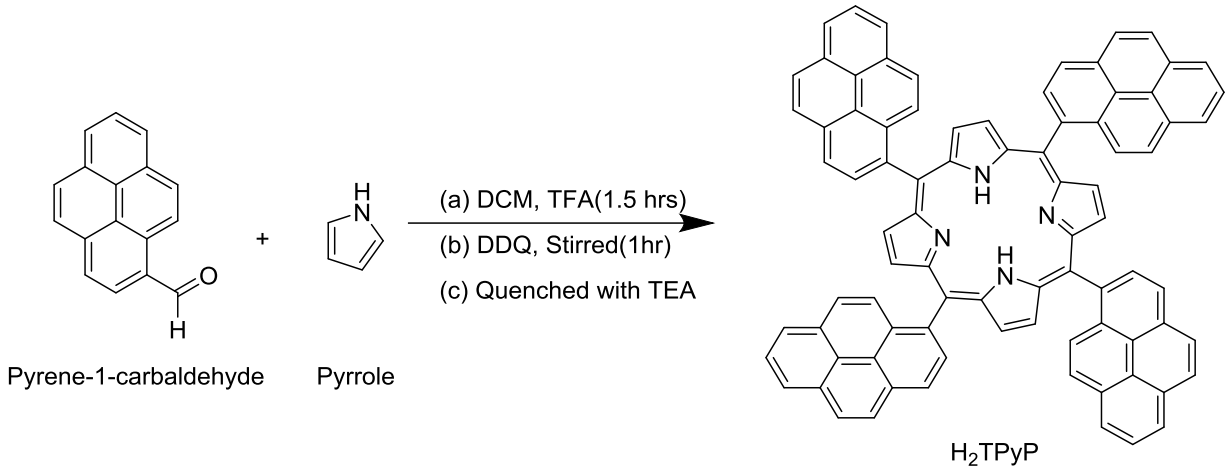

Scheme 4.2: Synthesis of H_2TPyP

The soret band of H_2TPyP was observed at 431 nm while the Q bands were observed at 520, 555, 595 and 655 nm consistent with a porphyrin derivative chromophore (Gouterman, 1961). Mass spectral data obtained for the compound showed the parent ion peak at 1111.302 $[M+H]^+$, calculated 1110.37, Appendix B.1, for $C_{84}H_{46}N_4$. The elemental analysis data (%) showed that the CHN composition of H_2TPyP was: C (90.38), H (4.13), N (4.98), in agreement with the molecular formula. The ^1H NMR spectrum showed a singlet at δ_H -2.40 (*s*, 2H) which was assigned to the highly shielded protons on the nitrogen bound pyrrole protons, (Bajju *et al*., 2013), Appendix B.2. The aromatic β-pyrrole and *meso*-pyrenyl (aryl) protons of H_2TPyP resonated in the aromatic region at δ_H 8.91 – 7.44 (*m*, 44H) in agreement with literature (Zoltan *et al*., 2010).

4.1.3 ZnTPyP

ZnPyP was prepared by reacting the freebase H_2TPyP with zinc acetate at room temperature conditions in DCM/MeOH (3:1) which gave a yield of 93%, Scheme 4.3.

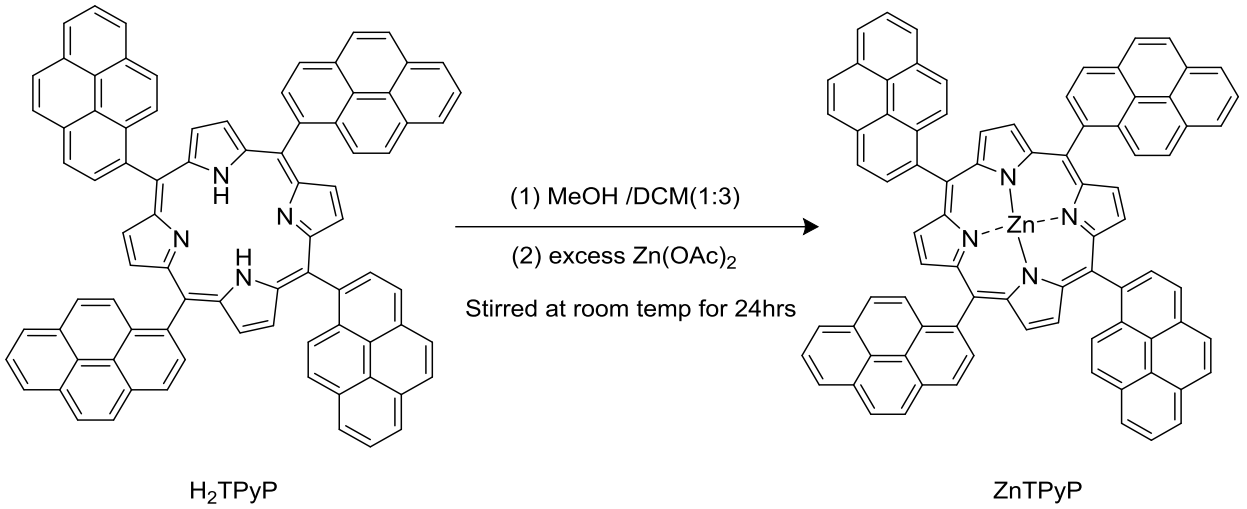

Scheme 4.3: Synthesis of ZnTPyP

The UV-Vis spectrum of ZnTPyP indicated that this compounds is a metalloporphyrin derivative: soret band (439 nm), Q bands (562, 603 nm), (Bajju *et al*., 2013). Unlike free base porphyrins which have 4 Q bands, metalloporphyrins have only two Q bands due to increase in symmetry (Bajju *et al*., 2013; Bajju *et al*., 2014). The mass spectral data obtained for the compound show the parent ion peak at 1173.673 $[M+H]^+$, calculated 1172.29, Appendix C.1 for $C_{84}H_{44}N_4Zn$. The elemental analysis data (%) showed that the CHN composition of ZnTPyP was: C (85.62), H (3.81), N (4.53) in agreement with its molecular formula. In the ^1H NMR spectrum of this compound, Appendix C.2, the signal associated with nitrogen bound protons (N-H) of pyrrole collapsed indicating the successful insertion of a zinc metal in porphyrin macrocycle (Bajju *et al*., 2013). Just as in H_2TPyP, the aromatic β-pyrrole and *meso*-pyrenyl (aryl) protons of ZnPyP resonated as multiplets in the aromatic region at δ_H 8.92 – 7.48 (*m*, 44H) (Zoltan *et al*., 2010; Bajju *et al*., 2013).

4.1.4 GaClTPyP

GaClTPyP was prepared by reacting freebase H_2TPyP with gallium (III) chloride in refluxing toluene to give a yield of 81%. Scheme 4.4.

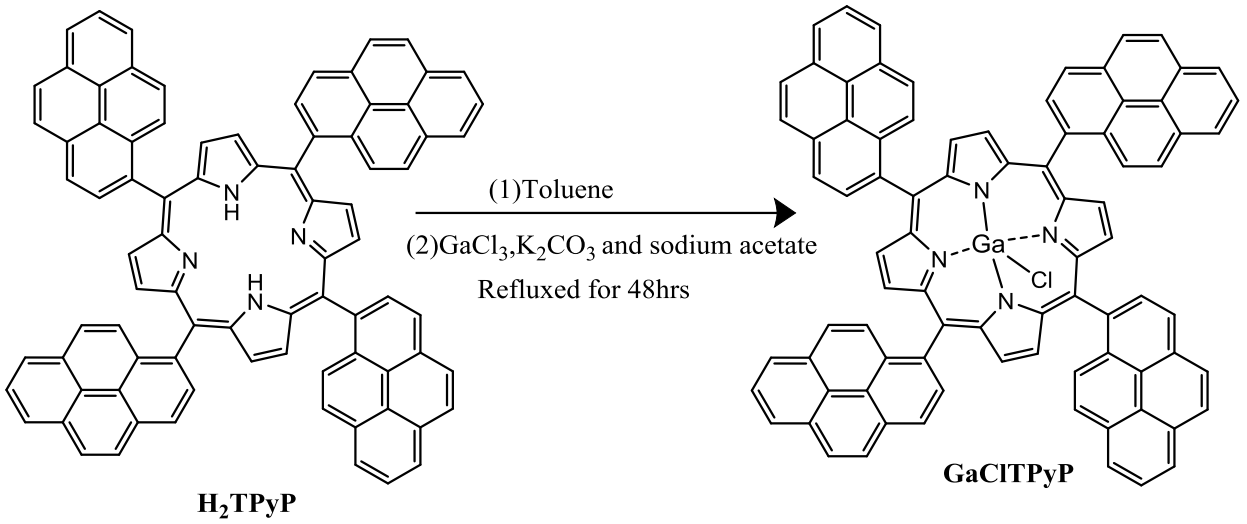

Scheme 4.4: Synthesis of GaClTPyP

The UV-Vis spectrum of GaClTPyP indicated that this compounds is a metalloporphyrin derivative: soret band (440 nm), Q bands (563 and 605 nm) (Bajju *et al*., 2013; Bajju *et al*., 2014). The mass spectral data showed peaks at 1178.513 and 1109.574 which was assigned to removal of Cl^- and Ga respectively, Calculated 1212.25. Appendix D.1 for $C_{84}H_{44}ClGaN_4$. The elemental analysis data (%) showed that the CHN composition of GaClTPyP was: C (83.14), H (3.48), N (4.29), which is in agreement with its molecular formula. In the ^1H NMR spectrum of this compound, the signal associated with nitrogen bound protons (N-H) of pyrrole collapsed indicating the insertion of the metal in porphyrin macrocycle. The aromatic β-Pyrrole and *meso*-pyrenyl (aryl) protons of GaClTPyP resonated in the aromatic region at δ_H 8.92 – 7.55 (*m*, 44H), slightly shifted compared to H_2TPyP, again supporting the metal insertion, Appendix D.2.

4.1.5 InClTPyP

InClTPyP was prepared by reacting freebase H_2TPyP with indium (III) chloride in refluxing acetic acid to give a yield of 87%. Scheme 4.5.

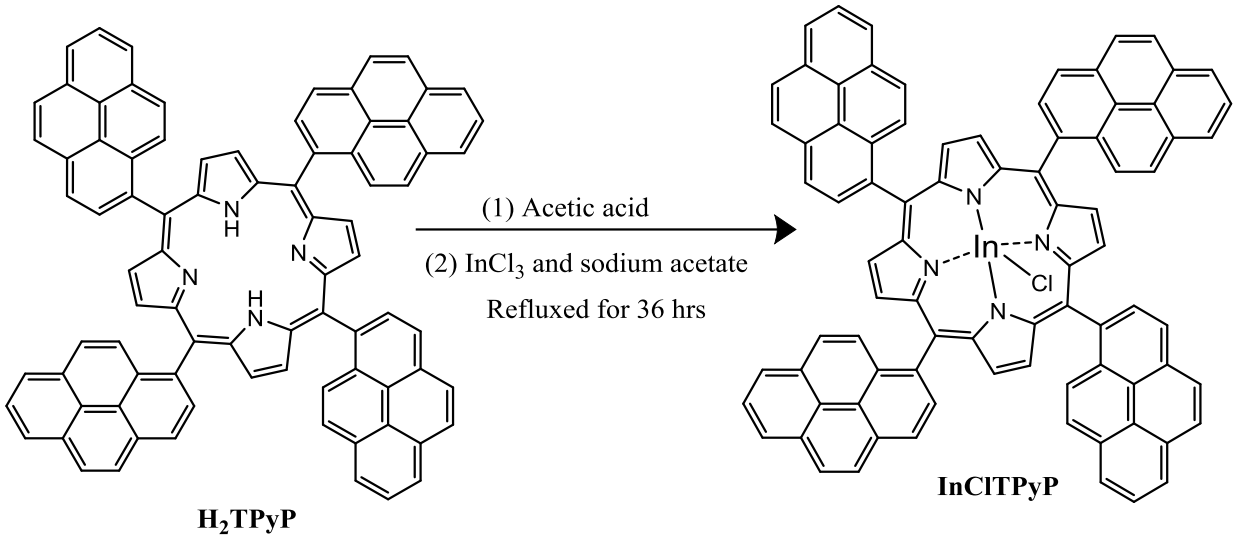

Scheme 4.5: Synthesis of InClTPyP

The UV-Vis spectrum of InClTPyP indicated that this compounds is a metalloporphyrin derivative: soret band (443 nm) and the Q bands (571 and 611 nm), (Bajju *et al*., 2013; Bajju *et al*., 2014). The mass spectral data obtained for the compound showed the parent ion peak at 1259.418 $[M+H]^+$, calculated 1258.23, Appendix E.1, for $C_{84}H_{44}ClInN_4$. The prominent peak at 1224.44 in the spectra was assigned to the removal of Cl^- from $[M+H]^+$, Appendix E.1. The elemental analysis data (%) showed that the CHN composition of InClTPyP was: C (79.98), H (3.47), N (4.39), in agreement with its molecular formula. In the ^1H NMR spectrum of this compound, the signal associated with nitrogen bound protons (N-H) of pyrrole collapsed indicating the successful insertion of indium metal in porphyrin macrocycle. The aromatic β-pyrrole and *meso*-pyrenyl (aryl) protons of InClTPyP resonated as multiplets in the aromatic region at δ_H 8.96 – 7.46 (*m*, 44H), Appendix E.2, slightly shifted compared to H_2TPyP again supporting the metal insertion (Zoltan *et al*., 2010; Bajju *et al*., 2013).

4.2 Photophysical Studies

The objective of this study was to synthesize bathochromically shifted porphyrin derivatives. Furthermore, this study's aim was to obtain porphyrin derivatives that are able to experience intersystem crossing to the triplet state. Subsequently, the exited triplet state photosensitizer is able to induce production of reactive oxygen species (ROS) namely free radicals (type I reaction) and singlet oxygen (type II reaction) by reacting with molecular oxygen (Moan and Berg, 1992;

Porfirinas and Fotodin, 1996). These ROS are lethal to cells and are the ones responsible for PACT activities (Moan and Berg, 1992). The parameter used to determine if the compounds were bathochromically shifted was UV-Vis spectroscopy. Fluorescence quantum yield (ϕ_F**)** which is measured using fluorescence spectroscopy is employed in this study to examine the emission properties of the synthesized compounds (Fery-Forgues and Lavabre, 2009). The ϕ_F gives the efficiency by which compounds are able to undergo intersystem crossing to the triplet state. Photosensitizers with low fluorescence quantum yield are efficient in intersystem crossing to the triplet state (Serevičius *et al*., 2017).

4.2.1 UV-Spectroscopy

The UV-Vis spectra of the synthesized compounds were measured and compared with the unsubstituted standard tetraphenylporphyrin (TPP). The soret band in porphyrin H_2TBrPP was bathochromically shifted by 5 nm while in H_2TPyP it was bathochromically shifted by 16 nm in comparison with tetraphenylporphyrin (TPP) as shown in Table 4.1. This illustrated that substituting the phenyl ring with the highly conjugated pyrene considerably changed the electronic properties of the porphyrin. This change was attributed to decrease in HOMO-LUMO gap with the increase in extended π conjugation in H_2TPyP (Detert *et al.,* 2010). The slight 5 nm shift observed in free base H_2TBrPP was attributed to electron withdrawing bromine groups being present around the porphyrin ring. This pulls electron density from the porphyrin ring, lowers the energy of the non-degenerate HOMOs and splits the energy of the degenerate LUMO pairs thereby reducing the HOMO-LUMO gap (Prakash *et al*., 2015; Zhang *et al*., 2017). This is what resulted in the slight bathochromic shift observed in H_2TBrPP. The bands that lie between $315 - 370$ nm in the UV-Vis spectra of H_2TPyP are associated to the presence of the pyren-1-yl groups.

A compound with a high molar extinction coefficient absorbs photons efficiently, hence more ground state electrons are exited (Yoon *et al.*, 2013). However, for the synthesized free-bases, the molar extinction coefficient at the peak position for H_2TPyP decreased to a value of 306,900 M^{-1} cm^{-1} from 372,500 in TPP. This is consistent with the effect of presence of pyrenyl groups within the porphyrin. There is ground state interaction between electro-active components within the pyrenyl group leading to reduction in molar absorptivity of absorption band in the UV-Vis spectrum (Mathew and Johnston, 2009; Hungerford *et al*., 2001; Wu *et al*., 2011).

Upon metallation of the ligand H_2TPyP with metals zinc, gallium and indium there was a striking spectral change. The four less intense Q bands in the free base porphyrin ligand of H_2TPyP collapsed into two, Figure 4.2. This was due to the change in symmetry upon metallation (Bajju *et al*., 2013). H_2TPyP has a D_{2h} symmetry due to the two hydrogen atoms on the diagonally located pyrollic nitrogen's (Arnaut, 2011; Bajju *et al*., 2013; Bajju *et al*., 2014). The corresponding metal conjugates has a D_{4h} symmetry and this increase in symmetry occasioned the decline in the number of absorption bands (Bajju *et al*., 2014).

In addition, comparing the free-base porphyrin ligand H_2TPyP spectrum with the metallated ZnTPyP, GaClTPyP and InClTPyP, a bathochromic shifting of the soret band was notable, Figure 4.2. This was because in a metallated porphyrin, there is a delocalized π system that allows free electron flow increasing electron density in metallo-porphyrins. The delocalized π system emanates from the metal ion at the core accepting lone pair of electrons from pyrrolic nitrogens in the porphyrin ring, while concurrently donating electrons to the porphyrin macrocycle (Zheng *et al.,* 2008). This results to increase in electron density in metallo-porphyrin as compared to the free-base thus reducing the HOMO-LUMO gap and subsequent energy of electron transition which is vital in the observed bathochromic shift of soret band (Zheng *et al.,* 2008). The progressive increase in soret band bathochromic shift for metallated porphyrin results from addition of electrons from (zinc < gallium < indium) leading to progressive reduction in the energy gaps (Zheng *et al.,* 2008).

Table 4.1: UV-Vis data for the synthesized porphyrin.

Compound	**UV-Vis Absorption data [λ_{max} nm ($\varepsilon\times10^4$ $M^{-1}cm^{-1}$)]**				
	Soret	**$Q_{Y(0,1)}$**	**$Q_{Y(0,0)}$**	**$Q_{X(0,1)}$**	**$Q_{X(0,0)}$**
H_2TPP	415(37.25)	498(0.843)	535(0.785)	574(0.556)	634(0.397)
H_2TBrPP	420(38.45)	515(0.892)	550(0.791)	585(0.391)	650(0.199)
H_2TPyP	431(30.69)	520(0.995)	555(0.537)	595(0.469)	655(0.215)
ZnTPyP	439(23.42)	562(1.354)		603(0.4963)	
GaClTPyP	440(20.73)	563(1.288)		605(0.4377)	
InClTPyP	443(19.95)	571(1.293)		611(0.4093)	

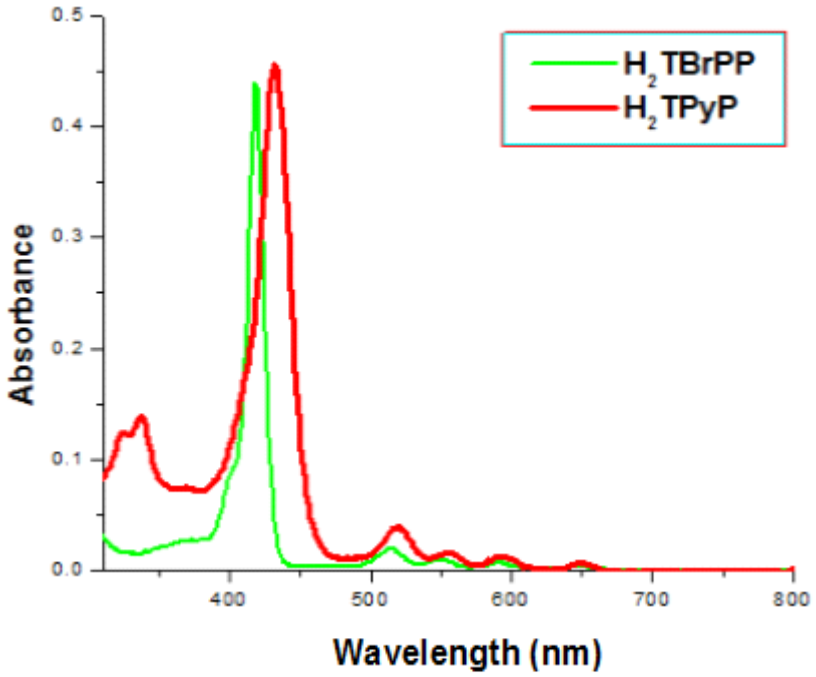

Figure 4.1: Normalized UV-Vis spectra for free base porphyrins

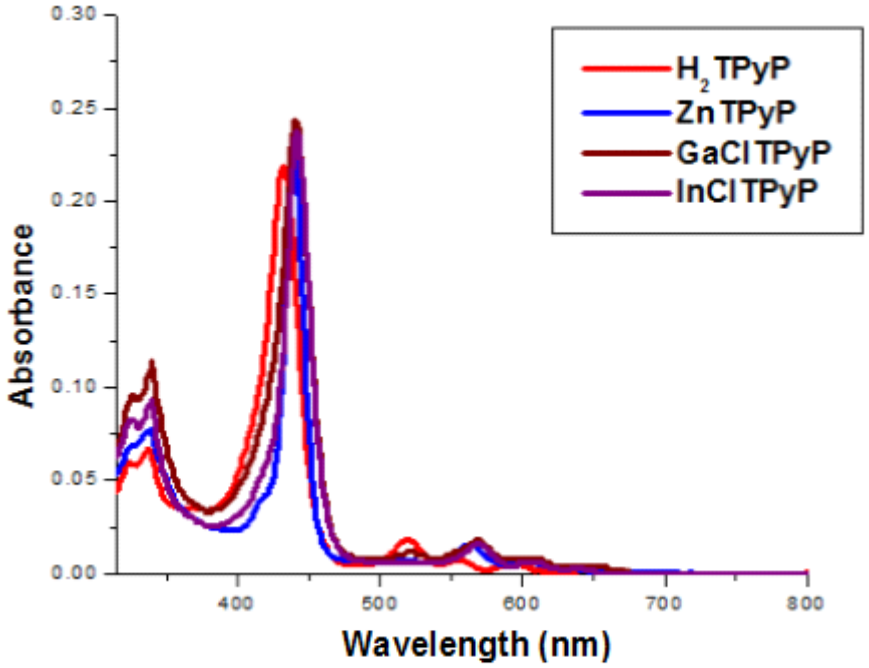

Figure 4.2: Normalized UV-Vis spectra for the metallated porphyrins

4.2.2 Fluorescence Spectroscopy

The fluorescence spectra of all the synthesized compounds showed identical shapes of two emission peaks with wavelength maxima between 649 – 662 and 715 – 726 nm, resulting from the soret band ($S_2 \rightarrow S_0$) and Q bands ($S_1 \rightarrow S_0$) transitions (Bajju *et al*., 2014), Figure 4.3 and 4.4. As shown in Table 4.2, a large stokes shift (λ = 206 – 295 nm) was obtained for all the synthesized compounds. The large stokes shift eliminates overlap between absorption and emission spectra, minimizes interference and allows for efficient detection of fluorescence (Gao *et al*., 2017; Ren *et al*., 2018).

The fluorescence quantum yield for H_2TPyP (0.133) was slightly higher than that recorded for the standard TPP (0.11) in DMF, Table 4.2. This is attributed to the highly π conjugated pyrene substituent present in the *meso* position of H_2TPyP (Ventura *et al*., 2007). A higher degree of π conjugation results to a high conformation stability of the exited states, longer lifetime and decrease in non-radiative decay constant that is often favorable for higher fluorescence quantum yield (Ventura *et al*., 2007; Yamaguchi *et al*., 2008).

Upon metallation, there was considerable decline in fluorescence quantum yield of corresponding metal conjugates zinc, gallium and indium when compared to their free base porphyrin H_2TPyP, Table 4.2. This behavior displayed by porphyrins on metallation was ascribed to reinforced spin-orbit coupling arising from the presence of heavy atom (Ji *et al.,* 2015; Knör and Strasser, 2002). This results to more streamlined intersystem crossing from porphyrin singlet exited state to the corresponding triplet exited state thus reducing probability of fluorescence emission. The impact of heavy atom is commensurable to Z^4 (Z = atomic number) thus the larger heavy atom effect in metallated indium porphyrin compared to zinc and gallium (Ji *et al.,* 2015; Knör and Strasser, 2002).

Table 4.2: Fluorescence data for the synthesized porphyrin.

Compound	Soret (λ_{max} nm)	Emission (λ_{max} nm)		Area	Quantum Yield (ϕ_F)	Stokes Shift (nm)
H_2TPP	415	648	712	2698352	0.110	233, 297
H_2TBrPP	420	652	717	2729706	0.112	232, 297
H_2TPyP	431	662	726	2421961	0.131	231, 295
ZnTPyP	439	656	722	291464	0.039	217, 283
GaClTPyP	440	655	720	333072	0.041	215, 280
InClTPyP	443	649	715	205980	0.017	206, 272
ZnTPP	422	651	714	546592	0.033	229, 292

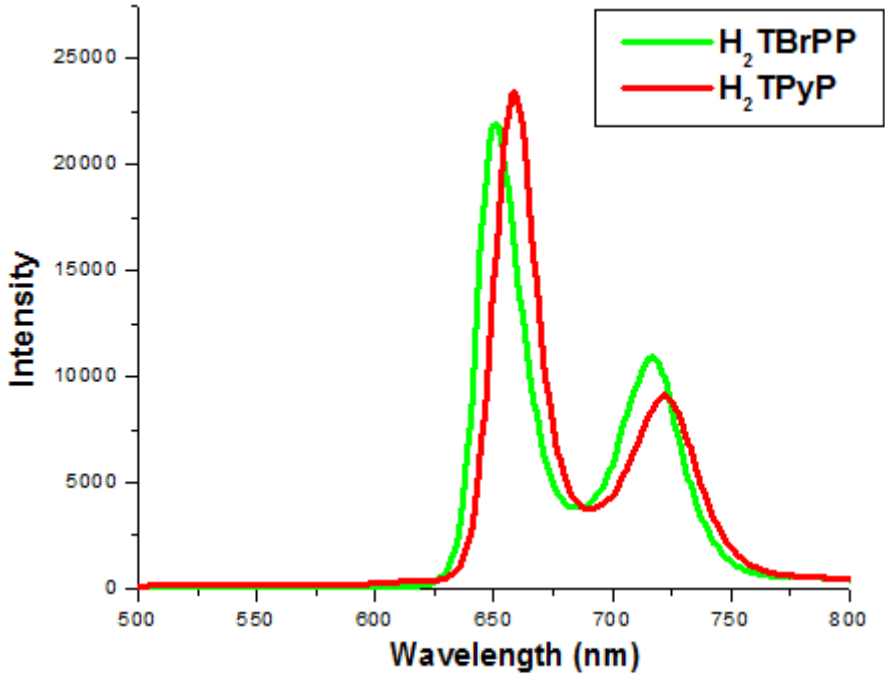

Figure 4.3: Normalized fluorescence emission spectra for free-base porphyrin.

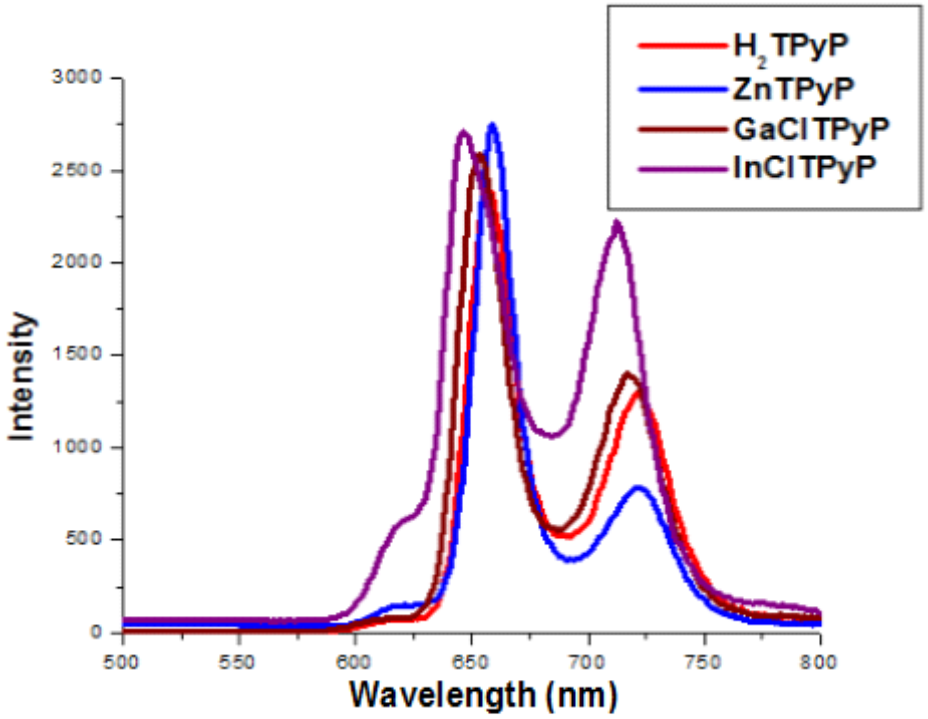

Figure 4.4: Normalized fluorescence emission spectra for the metallated porphyrin

The results from the photophysical studies showed that, by extending the conjugation through the presence of pyren-1-yl group in H_2TPyP results to bathochromic shifting in the absorption wavelength. Upon metallation of free-base H_2TPyP, further bathochromic change in the soret band of the metalloporphyrin was noted and the four less intense Q bands in the freebase collapsed to two. In addition to this, metallation of H_2TPyP enhanced intersystem transition to the triplet exited state owing to the impact of the heavy atom as shown from the values of fluorescence quantum yield obtained. Indium porphyrin displayed a larger heavy atom effect than zinc and gallium porphyrin conjugates due to its higher atomic number.

4.3 Antimicrobial Studies

The main purpose of synthesizing and characterizing the different porphyrin derivatives was to determine their prospective application in photodynamic antimicrobial therapy (PACT). To achieve this, the synthesized freebases and the corresponding metalloporphyrins antimicrobic activities were examined against the gram positive bacteria *Staphylococcus aureus* at different concentrations in presence (light) and absence (dark) of light. This study was important because when a photosensitizer molecule absorbs light, it moves from stable ground state to either singlet

excited state or can undergo intersystem crossing to the triplet excited state (Moan and Berg, 1992). The triplet excited state has longer lifetime than singlet excited state hence more time to react with other molecules in the environment such as molecular oxygen to produce reactive oxygen species (ROS) and radical ions, which in the case of PACT destroys microbial cells (Moan and Berg, 1992; Sternberg *et al*., 1998). Furthermore, it is important for a compound to be used as a photosensitizer in PACT to have low dark toxicity hence for this study dark toxicity studies were done to ascertain that the antimicrobial activity of the compounds were due to photo-toxicities and not as a result of toxic properties of the compounds (Porfirinas and Fotodin, 1996).

The results for the antimicrobial assay of the synthesized porphyrins at different concentrations in the presence of white light showed effective dose dependent photoinactivation effect against the bacteria *Staphylococcus aureus*, Figures 4.5 - 4.8. Among the free bases tested H_2TBrPP displayed low photoinactivation activity with IC_{50} of 49.57 µM, Figure 4.5, while H_2TPyP (Figure 4.6) displayed relatively good photoinactivation activity with IC_{50} of 27.89 µM. This is attributed to the enhanced singlet oxygen generating ability of porphyrin H_2TPyP due to the presence of *meso* pyrenyl group (Mananga, 2017; Zoltan *et al*., 2010). Metallated porphyrin ZnTPyP (Figure 4.7) and InClTPyP (Figure 4.8) exhibited relatively pronounced photoinactivation effect with an IC_{50} of 12.9 and 16.67 µM, respectively. Compared to the free bases, the metallated porphyrins displayed good photoinactivation activity even at low concentration, Figure 4.9. This was attributed to heavy atom effect upon metallation of the free base H_2TPyP (Ji *et al.*, 2015; Knör and Strasser, 2002). Metallation can enhance the photoinactivation process by efficient intersystem crossing from porphyrin singlet exited state to the corresponding triplet state thus reducing incidence of fluorescence emission and increasing the generation of ROS (Mthethwa and Nyokong, 2015). These results are consistent with the quantum yield results, Section 4.2.2, which theoretically suggest in terms of PACT activities the order should be InClTPyP > ZnTPyP > H_2TBrPP > H_2TPyP. However, ZnTPyP had the highest PACT activities due to the natural antimicrobial properties of zinc against bacteria (McDevitt *et al*., 2011; Yasuyuki *et al.*, 2010), Figure 4.9. Dark toxicity results for all the tested photosensitizers showed no significant effect on cell viability, Figures 4.5 - 4.8.

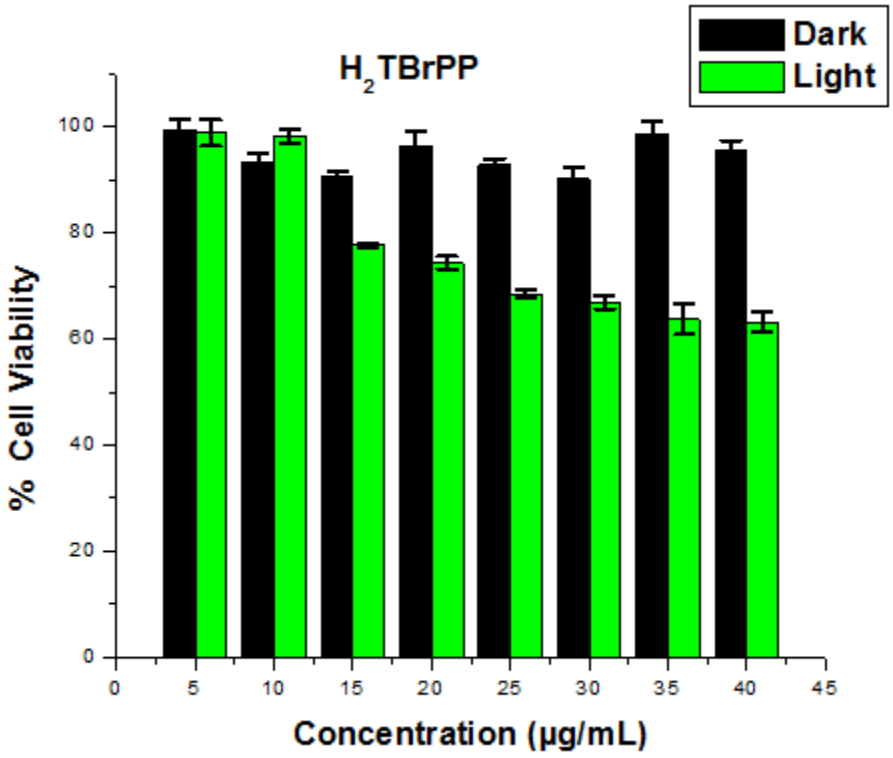

Figure 4.5: Antimicrobial activity of H_2TBrPP in the presence and absence of light

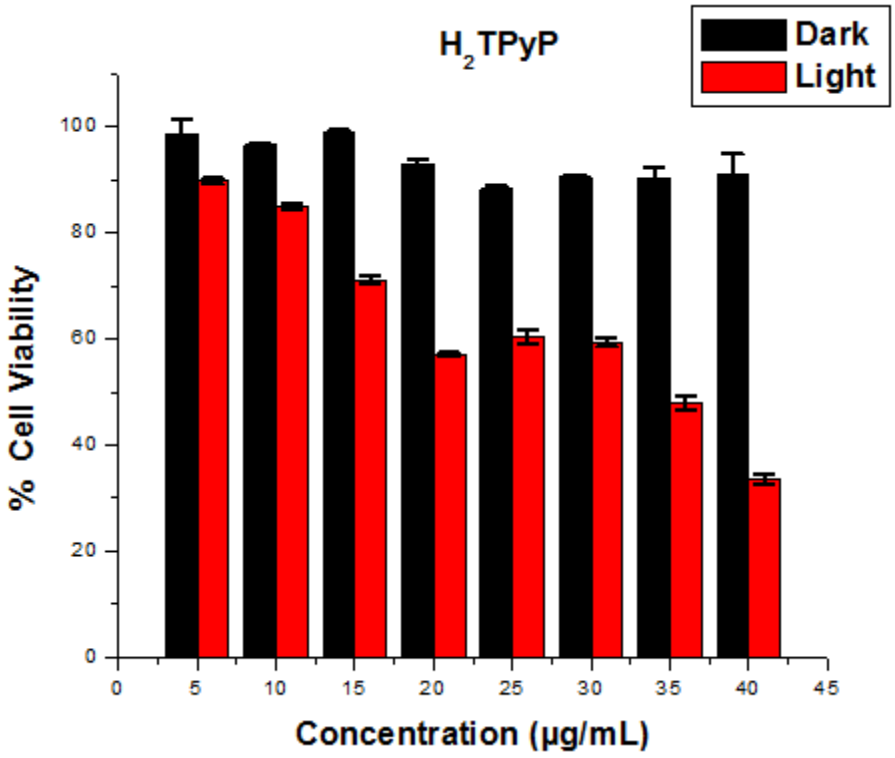

Figure 4.6: Antimicrobial activity of H_2TPyP in the presence and absence of light

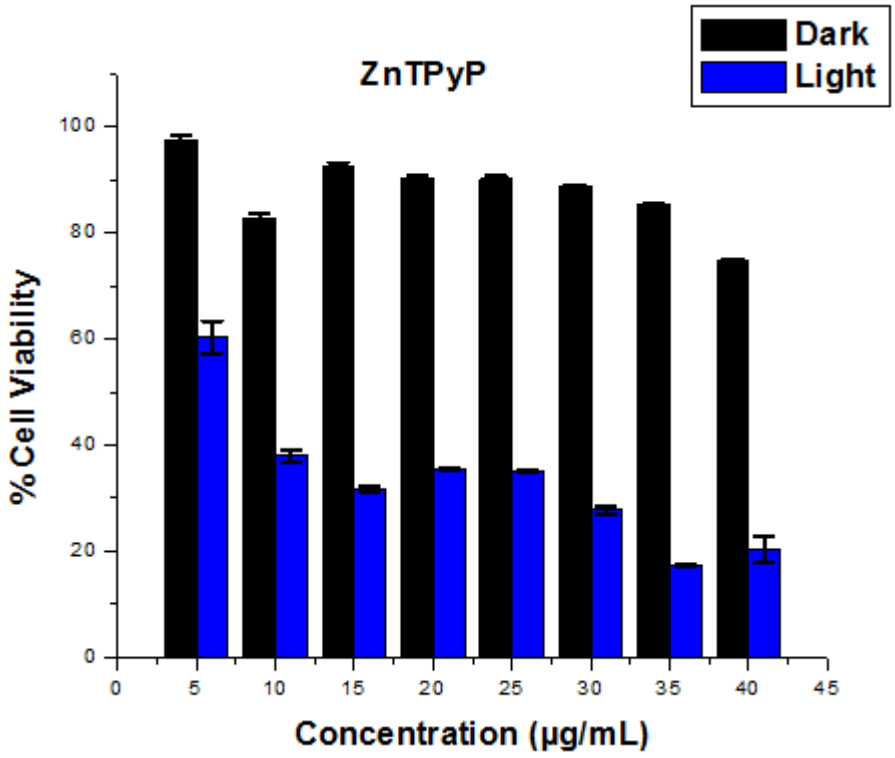

Figure 4.7: Antimicrobial activity of ZnTPyP in the presence and absence of light

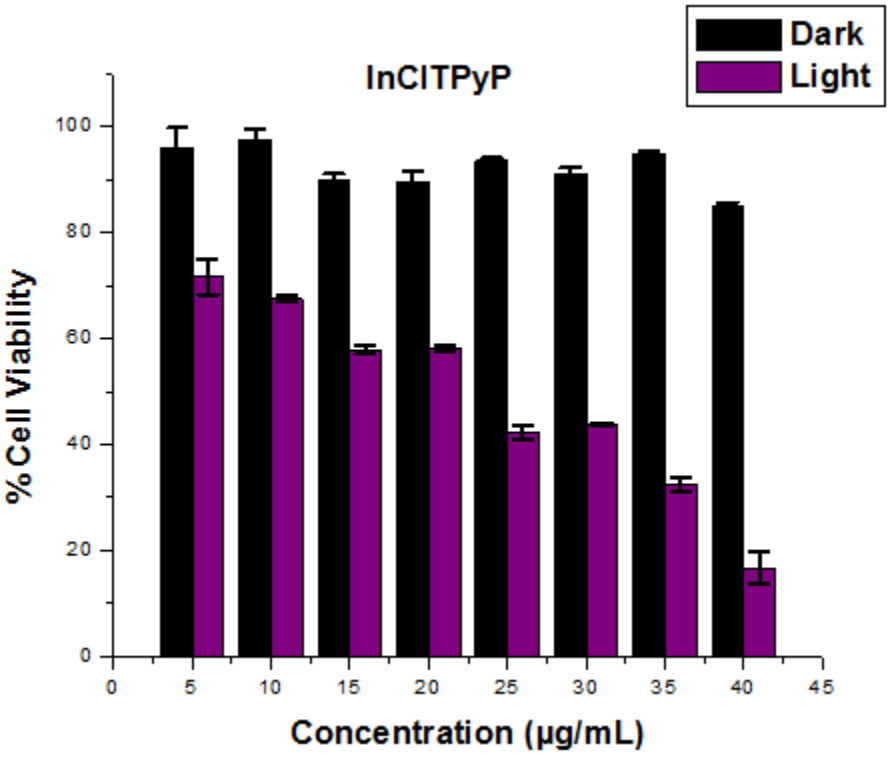

Figure 4.8: Antimicrobial activity of InClTPyP in the presence and absence of light

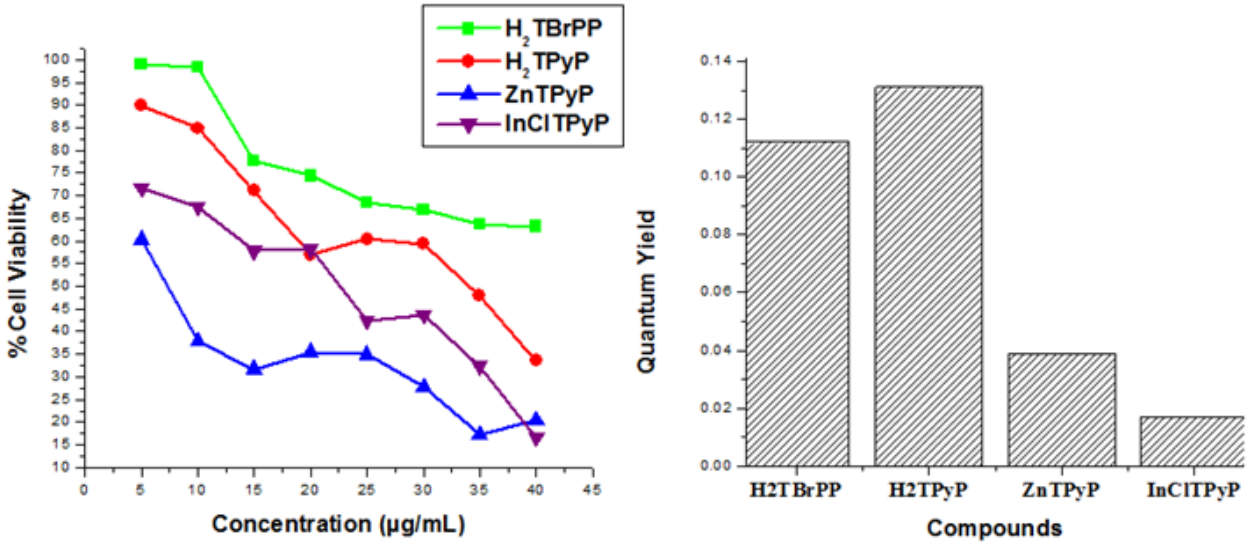

Figure 4.9: Comparison of % cell viability at different concentration and fluorescence quantum yield

CHAPTER FIVE
CONCLUSIONS AND RECOMMENDATIONS

5.1 Conclusions

The conclusions drawn from the study are:

1. Five compounds were successfully synthesized and characterized on the basis of UV-Vis absorption, CHN elemental analysis, ^{1}H NMR spectroscopy and mass spectrometry data. The five compounds comprised of two free base porphyrins H_2TBrPP and H_2TPyP. The free base of H_2TPyP was metallated with metal zinc, gallium and indium to synthesize the corresponding ZnTPyP, GaClTPyP and InClTPyP metalloporphyrins respectively. This is the first synthesis of InClTPyP and is novel.
2. Upon metallation, the photophysical properties of the synthesized compounds improved. There was bathochromic shifting of absorption maxima and reduction of quantum yield. Of the five compounds synthesized, InClTPyP was the most bathochromically shifted (28 nm) compared to standard TPP.
3. PACT studies revealed that all the compounds showed effective dose dependent inhibition against S*taphylococcus aureus.* Metallated ZnTPyP and InClTPyP provide more pronounced photoinactivation effect. The results in this work demonstrated that the synthesized compounds have potential utility for application in PACT.

5.2 Recommendations

This study recommends the following:

1. The synthesized compounds: H_2TBrPP, H_2TPyP, ZnTPyP, GaClTPyP and InClTPyP should be tested against other microorganisms.
2. ZnTPyP and InClTPyP that exhibited pronounced photoinactivation effect can be immobilized on solid support for application in PACT.
3. Modification of the synthesized metalloporphyrins by axial ligation to help improve photophysical and antimicrobial properties.

REFERENCES

Allison, R. R., Downie, G. H., Cuenca, R., Hu, X. H. and Sibata, C. H. (2004). Photosensitizers in clinical PDT. *Photodiagnosis and Photodynamic Therapy, 1,* 27–42.

Adler, A. D., Longo, F. R., Finarelli, J. D., Goldmacher, J., Assour, J., and Korsakoff, L. (1967). A Simplified Synthesis for *Meso*-Tetraphenylporphine. *Journal of Organic Chemistry, 32(2),* 476.

Amuhaya, E., (2011). *Synthesis, Biological and Photophysical Studies of Novel Compounds for Cancer Therapy.* PhD Thesis, Louisiana State University. pp. 161.

Arnaut, L. G. (2011). Design of porphyrin-based photosensitizers for photodynamic therapy. *Advances in Inorganic Chemistry, 63,* 187–233.

Bajju, G. D., Anand, S., Kundan, S. and Singh, N. (2013). Electrochemical and Spectroscopic Characterization of Aluminium(III)-para-methyl-meso-tetraphenylporphyrin Complexes Containing Substituted Salicylates as Axial Ligands. *International Journal of Electrochemistry 10,* 1–10.

Bajju, G. D., Kundan, S., Bhagat, M., Gupta, D., Kapahi, A., and Devi, G. (2014). Synthesis and Spectroscopic and Biological Activities of Zn (II) Porphyrin with Oxygen Donors. *Bioinorganic Chemistry and Applications 2,* 1–13.

Bhatti, M. & Mast, E. (1972). Preparation of Indium(III)tetraphenylporphyrin complexes. *Inorg.Nuc. Chem. 8,* 133–137.

Bharadwaj, J. and Sharma, A. (2016). Detection of *Escherichia Coli, Staphylococcus aureus* and *Salmonella Typhi* in drinking water in Governmental instituitions and organizations of Gwalior City. *IJESRT 5(7),* 769–774.

Brookfield, B. Y. R. L. (1985). Luminescence of Porphyrins and Metalloporphyrins. *J. Chem. Soc., Faraday Trans. 82(2),* 1837–1848.

Carvalho, C. M. B., Gomes, A., Fernandes, S. C. D., Prata, A. C. B., Almeida, M. A., Cunha, M. A., Tome´, J. P. C., Faustino, M. A. F., Neves, Maria, G. P. M. S., Tome´, A. C., Cavaleiro, J. A. S., Zhi Lin., Rainho, J. P. and Rocha, J. (2007). Photoinactivation of Bacteria in Wastewater by Porphyrins: Bacterial β-Galactosidase Activity and Leucine-Uptake as Methods to Monitor the Process. *Journal of Photochemistry and Photobiology 88,* 112–118.

Cavaleiro, J. and Smith, K. (1987). Protoporphyrin-IX: Some Useful Substituent Manipulations. *Heterocycles 26*(7), 1947–1963.

Centre for Disease Control and Prevention (CDC) (2012). Solar Disinfection. Retrieved October 30, 2019 from https://www.cdc.gov/safewater/solardisinfection.html

Centre for Disease Control and Prevention (CDC) (2014a). Drinking water diseases and contaminants. Retrieved October 26, 2019 from https://www.cdc.gov/healthywater/drinking/public/water_diseases.html

Centre for Disease Control and Prevention (CDC) (2014b). *Escherichia Coli* (*E.Coli*). Retrieved November 26, 2019 from https://www.cdc.gov/ecoli/index.html

Chevalier, F., Geier, G. R., & Lindsey, J. S. (2002). Acidolysis of intermediates used in the preparation of core-modified porphyrinic macrocycles. *Journal of Porphyrins and Phthalocyanines, 6*(3), 186–197.

Chambers, H. F. and Deleo, F. R. (2010). Waves of Resistance: *Staphylococcus aureus* in the Antibiotic Era. *Nat Rev Microbiol, 7*(9), 629–641.

Chang, Y. , Yang, C. , Sun, R. , Cheng, Y. , Kao, W. and Yang, P. (2013). Rapid single cell detection of *Staphylococcus aureus* by aptamer-conjugated gold nanoparticles. *Sci. Rep. 3,* 1–7.

Deda, D. K. and Araki, K. (2015). Photosensitizers in medicine. *J. Braz. Chem. Soc., 26*(12), 2448-2470.

Detert, H., Lehmann, M. and Meier, H. (2010). Star-shaped conjugated systems. *Materials. 3*(5), 3218–3330.

Dobson, J. and Wilson, M. (1992). Sensitization of Oral Bacteria in Biofilms to Killing by light from a Low-Power Laser. *Archs Oral Bio, 37*(11), 883–487.

Enviroment Protecting Agency (EPA) (2017). Contaminant Candidate List (CCL) and Regulatory Determination. Retrieved January 3, 2019 from https://19january2017snapshot.epa.gov/ccl/types-drinking-water-contaminants_.html

Falvo, R. E., Mink, M. L. and Marsh, D. F. (1999). Microscale Synthesis and ^{1}H NMR Analysis of Tetraphenylporphyrins. *Journal of Chemical Education. 76*(2), 237–239.

Fery-Forgues, S. and Lavabre, D. (2009). Are Fluorescence Quantum Yields So Tricky to Measure? A Demonstration Using Familiar Stationery Products. *J. Chem. Educ., 76*(9), 1260.

Foote, S. C., (1991). Definition of Type I and Type II photosensitized Oxidation. *Photochemistry and Photobiology 54*(5), 659.

Gao, Z., Hao,Y. and Zheng, M. (2017). A fluorescent dye with large stokes shift and high stability:

synthesis and application to live cell imaging. *RSC 7*, 7604-7609.

Grinholc, M. and Bielawski, K. P. (2008). Bactericidal effect of photodynamic inactivation against methicillin-resistant and methicillin-susceptible *Staphylococcus aureus* is strain-dependent. *J. Photochem. Photobiol. B Biol. 90*, 57–63.

Gouterman, M., (1961). Spectra of Porphyrins. *J. Mol. Spec. 6*, 138–163.

Gouterman, M., Wagnière, G. H., & Snyder, L. C., (1963). Spectra of Porphyrins: Part II Four Orbital Model. *J. Mol. Spec*. *11*, 108–127.

Gwimbi, P., George, M. and Ramphalile, M. (2019). Bacterial contamination of drinking water sources in rural villages of Mohale Basin, Lesotho: exposures through neighborhood sanitation and hygiene practices. *Environmental Health and Preventive Medicine*, *24*, 33.

Hamblin R. M., and Jori G. (2011). *Photodynamic Inactivation of Microbial Pathogens:Medical and Enviromental Application*. Cambridge, U.K:Royal Society of Chemistry. pp 434.

Huang, X., Nakanishi, K., and Berova, N. (2000). Porphyrins and Metalloporphyrins : Versatile Circular Dichroic Reporter Groups for Structural Studies. *Chirality 12*, 237–255.

Hungerford, G., Auweraer, M. and Amabilino, D. B. (2001). Intramolecular fluorescence quenching in porphyrin- bearing [2] catenates. *Journal of Porphyrins and Phthalocyanines*, *5*(8), 633–644.

Ji, S., Ge, J., Escudero, D., Wang, Z., Zhao, J., & Jacquemin, D. (2015). Molecular structure-intersystem crossing relationship of heavy-atom-free bodipy triplet photosensitizers. *Journal of Organic Chemistry*, *80(11)*, 5958–5963.

Jin, M., Liu, L., Wang, D., Yang, D., Liu, W., Yin, J. and Li, J. (2020). Chlorine disinfection promotes the exchange of antibiotic resistance genes across bacterial genera by natural transformation. *The ISME Journal 14*, 1847–1856.

Jodlbauer, A. and Tappainer, H. (1904). On the Participation of Oxygen in the Photodynamic effect of fluorescent substances, *Mu¨nch. Med. Wochenschr., 26*, 1139–1141.

Jori, G. and Brown, B. S. (2004). Photosensitized Inactivation of Microorganisms. *Journal of Photochemistry and Photobiology 3*, 403–405.

Karumathil, D. P., Yin, H., Johny, A. K., & Kumar, V. (2014). Effect of Chlorine Exposure on the Survival and Antibiotic Gene Expression of Multidrug Resistant *Acinetobacter baumannii* in Water. *Int. J Environ Res Public Health. 11*(2), 1844–1854.

Kenya Vision 2030 (2008). Kenya Vision 2030. Retrieved June 30, 2020 from http://vision2030.go.ke/inc/uploads/2018/05/Vision-2030-Popular-Version.pdf

Knör, G., & Strasser, A. (2002). Coexisting intraligand fluorescence and phosphorescence of hafnium(IV) and thorium(IV) porphyrin complexes in solution. *Inorganic Chemistry Communications*, *5*(11), 993–995.

Lindsey, J. S., Schreiman, I. C., Huasu, H. C., Kearney, P. C., and Marguerettaz, A. M. (1987). Rothemund and Adler-Longo Reactions Revisited: Synthesis of Tetraphenylporphyrins under Equilibrium Conditions. *Journal of Organic Chemistry*, *52*(5), 827–836.

Lindsey J.S. (1994). *The Synthesis of Meso-Substituted Porphyrins*. Springer; Dordrecht.

Lindsey, J. S., Maccrum, K. A., Tyhonas, J. S., & Chuang, Y. (1994). Investigation of Synthesis of *meso*-Porphyrins Employing High Concentration Conditions and an Electron Transport Chain for Aerobic Oxidation. *Journal of Organic Chemistry*, *32*(10), 828–836.

Lindsey, J. S. (2010). Synthetic routes to meso-patterned porphyrins. *Accounts of Chemical Research*. *43*(2), 300–311.

Llor, C. and Bjerrum, L. (2014). Antimicrobial resistance: risk associated with antibiotic overuse and initiatives to reduce the problem. *Therapeutic Advances in Drug Safety*, *5*(6), 229–241.

Lowy, F. D. (2003). Antimicrobial resistance : the example of *Staphylococcus aureus*. *J. Clin. Invest. 111*(9), 1265–1273.

Mananga, M., Britton, J. Amuhaya, E. and Nyokong, T. (2017). Photophysical properties of GaCl 5,10,15,20-tetra(1-pyrenyl) porphyrinato incorporated into Pluronic F127 micelle. *Journal of Luminescence 185*, 34–41.

Mantareva, V., Kussovski, V., Angelov, I., Borisova, E., and Avramov, L. (2007). Photodynamic activity of water-soluble phthalocyanine zinc (II) complexes against pathogenic microorganisms. *J. Bioorganic & Medicinal Chemistry 15*, 4829–4835.

Mark, W. L. and Ramon, J. S. (1980). *Staphylococcus aureus* in Rural Drinking Water. *J. Applied and Environmental Microbiology 30*(4), 739–742.

Mathew, S., and Johnston, M. R. (2009). The Synthesis and Characterisation of a Free-Base Porphyrin – Perylene Dyad that Exhibits Electronic Coupling in Both the Ground and Excited States. *Chemistry - A European Journal, 15*(1), 248–253.

McDevitt, C. A. (2011). A molecular mechanism for bacterial susceptibility to zinc. *PLoS Pathogen*, *7*(11), 1–8.

Merchat, M., Bertolini, G., Giacomini, P., Villanueva, A., and Jori, G. (1996). Meso-substituted cationic porphyrins as efficient photosensitizers of gram-positive and gram-negative bacteria. *Journal of Photochemistry and Photobiology B: Biology 32*, 153–157.

Moan, J. and Berg, K. (1992). Yearly Review Photochemotherapy Of Cancer : Experimental. *Photochemistry and Photobiology 55*(6), 931–48.

Mthethwa, T. and Nyokong, T. (2015). Photoinactivation of Candida albicans and Escherichia coli using aluminium phthalocyanine on gold nanoparticles. *Photochem. Photobiol. Sci*. *33*(3), 801–807.

Munita, J. M., and Arias, C. A. (2016). Mechanisms of Antibiotic Resistance. *Microbiol Spectr*. *4*(2), 1–37.

Neth, K. L. N., Carlin. M. C. and Keen, K.O. (2017). Doxycycline transformation and emergence of antibacterially active products during water disinfection with chlorine. *Environ.Sci.: Water Res. Technol., 3,* 1086–1094.

Okamoto, H., Tatsuo Iwase, D. and Toshio M. (1990). Dye-Mediated Bactericidal Effect of He-Ne Laser Irradiation on Oral Microorganisms. *Lasers in Surgery and Medicine 12,* 450–458.

Osifeko, O. L., Uddin, I., Mashazi, P. N. and Nyokong, T. (2016). Physicochemical and antimicrobial photodynamic chemotherapy of unsymmetrical indium phthalocyanines alone or in the presence of magnetic nanoparticles. *New J. Chem. 40*, 2710–2721.

Pandey, P. K., Kass, P. H., Soupir, M. L., Biswas, S., & Singh, V. P. (2014). Contamination of water resources by pathogenic bacteria. *AMB Express*, *4*(51), 1–16.

Pinchuk, I. V., Beswick, E. J. and Reyes, V. E. (2010). Staphylococcal enterotoxins. *Toxins 2*, 2177–2197.

Peeks, M. D., Timothy D. W., Claridge, M. and Harry L. A. (2017). Aromatic and antiaromatic ring currents in a molecular nanoring. *Phys.Chem. Phys. 18,* 1–16.

Porfirinas, A. and Fotodin, T. (1996). Porphyrins and the Photodynamic Therapy of Cancer**.** *Rey. Port. Quím.3*, 47–58.

Prakash, K., Kumar, R. and Sankar, M. (2015). Mono- and Tri-β-Substituted Unsymmetrical Metalloporphyrins: Synthesis, Structural, Spectral and Electrochemical Properties. *Royal Society of chemistry. 5*(82), 66824–66832.

Prestinaci, F., Pezzotti, P., and Pantosti, A. (2015). Antimicrobial resistance: a global multifaceted phenomenon. *Pathogens and Global Health, 109(7),* 309–318.

Raab, O. (1900). On the Effect of Fluorescein Substances and Infusoria, *Time for Biol., 39*, 524–546.

Rastodi, S. and Dwivedi, U. N. (2006). Biomolecules (Introduction, Structure and Functions) Porphyrin. University of Lucknow.

Raven, P. H. and Johnson, J. B. (2002). *Biology.* Boston; McGraw-Hill.

Ren, T., Xu, W., Zhang, W., Yuan, L. and Zhang, X. (2018). A general method to increase stokes shift by introducing Alternating vibronic structures. *Journal of the American Chemical Society, 140* (24), 7716–7722.

Rothemund, P., and Menotti, A. R. (1941). Porphyrin studies. IV.1The Synthesis of α,β,γ,δ-Tetraphenylporphine. *Journal of the American Chemical Society, 63*(1), 267–270.

Sekhar, C. K. P. (2013). *Synthesis and Biological Studies of Some Novel Porphyrin Appended Heterocycles.* PhD Thesis, Birla Institute of Technology and Science Pilani (Rajasthan). pp215.

Sekwadi, E., Ndip, R. and Bessong, P. (2015). Detection of Pathogenic *Escherichia Coli* and *Staphylococcus aureus* from cattle and pigs slaughtered in Abaltoirs in Vhembe District, South Africa. *Scientific World Jornal 195*(972), 1–8.

Serevičius, T., Komskis, O., Adomėnas, P., Adomėnienė, 0., Gediminas, K., Vygintas J. and Karolis K. (2017). Triplet–Triplet Annihilation in 9,10-Diphenylanthracene Derivatives: The Role of Intersystem Crossing and Exciton Diffusion. *J. Phys. Chem. 121*(15), 8515–8524.

Silva, S., Pereira, P. M. R. , Silva, P., Faustino, M. A. F. , Cavaleiro, J. A. S. and Tomé, J. P. C. (2012). Porphyrin and phthalocyanine glycodendritic conjugates: synthesis, photophysical and photochemical properties. *Chemical Communications*, *48*(30), 3608.

Solov, N., & Kachura, F. (1972). Spectra of porphyrins. *Physics*, *17*(5), 918–920.

Sternberg, E. D., Dolphin, D. and Brickner, C. (1998) Porphyrin based photosynthesizers for Use in Photodynamic Therapy.*Tetrahedron 54,* 4151–4202.

Straten, D. V., Mashayekhi, V., Bruijn, H., Oliveira, S., and Robinson, D. (2017). Oncologic Photodynamic Therapy: Basic Principles, Current Clinical Status and Future Directions. *Cancers*. *9(2),* 19.

Szãlkai, K. (2019). *Water-borne diseases.* Palgrave Macmillan, Cham.

Tanih, N., Sekwadi, E., Ndip, R. and Besong, P. (2015). Detection of *Escherichia coli* and *Staphylococcus aureus* from Cattle and Pigs slaughtered in Abattoirs in Vhembe District,

South Africa. *The scientific World Jornal*, *10*, 1–8.

Tavares, A., Carvalho, C. M. B., Faustino, M. A., Neves, G. P. M., João, P. C., Tomé, P. C. J., Tomé, A. C., Cavaleiro, J. A. S., Cunha, A., Gomes, N. C. M., Alves, E. and Almeida, A. (2010). Antimicrobial Photodynamic Therapy : Study of Bacterial Recovery Viability and Potential Development of Resistance after Treatment. *Mar. Drugs 8*, 91–105.

U.N. Water (2017). GLAAS report: Financing Universal Water, Sanitation and Hygiene under the Sustainable Development Goals. Retrieved October 30, 2019 from https://www.unwater.org/publications/un-water-glaas-2017-financing-universal-water-sanitation-hygiene-sustainable-development-goals/

U.N. Water (2019). Sustainable Development Goal 6 on water and sanitation (SDG 6). Retrieved August 30, 2019 from https://www.sdg6data.org/

U.N. General Assembly (28 July 2010). The human right to water and sanitation, A/RES/64/292. Retrieved October 25, 2019 from https://www.un.org/ga/search/view_doc.asp?symbol=A/RES/64/292.

Ventura, B., Flamigni, L., Marconi, G., Lodato, F., and Officer, D. L. (2008). Extending the porphyrin core: synthesis and photophysical characterization of porphyrins with π-conjugated β-substituents. *New J. Chem.*, *32*(1), *166–178.*

Vicente, M. G. H. (2001). Porphyrin-based Sensitizers in the Detection and Treatment of Cancer : Recent Progress. *Curr. Med. Chem. - Anti-Cancer Agents*. *23*(2), 175–194.

Wagnières, G. A, Star, W. M. and Wilson, B. C. (1998). In Vivo Fluorescence Spectroscopy and Imaging for Oncological Applications. *Photochemistry and Photobiology*. *68*(5), 603–632.

Weaver, J.J., (2005). *Corroles.* PhD Thesis, California Institute of Technology. pp 1–116.

Wilson, M., Burns,T., Pratten, J. and Pearson, G. J. (1995). Bacteria in Supragingival Plaque Samples Can Be Killed by Low-Power Laser Light in the Presence of a Photosensitizer. *Journal of applied Bacteriology 78*, 569–574.

World Health Organization (WHO) (2003*).* Emerging Issues Water and Infectious Disease. Retrieved December 10, 2018 from https://www.who.int/water_sanitation_health/publications/emergingissues/en/

World Health Organization (WHO) (2014). Antimicrobial Resistance: An Emerging Water, Sanitation and Hygiene Issue. Retrieved November 10, 2019 from https://apps.who.int/iris/handle/10665/204948

World Health Organization (WHO) (2015). Technical Briefing on Boil Water. Retrieved September 15, 2019 from https://www.who.int/water_sanitation_health/dwq/Boiling_water_01_15.pdf?ua=1&ua=1

World Health Organization (WHO) (2017a). 2.1 billion People lack safe drinking water at home, more than twice as many lack safe sanitation. Retrieved November 30, 2019 from https://www.who.int/news-room/detail/12-07-2017-2-1-billion-people-lack-safe-drinking-water-at-home-more-than-twice-as-many-lack-safe-sanitation

World Health Organization (WHO) (2017b). Guidelines for Drinking-water Quality*:* Fourth Edition incorporating the first addendum. Retrieved August 31, 2019 from https://apps.who.int/iris/bitstream/handle/10665/254637/9789241549950-eng.pdf?sequence=1

World Health Organization (WHO) (2018). *Escherichia Coli* (*E.Coli*). Retrieved November 16, 2019 from https://www.who.int/news-room/fact-sheets/detail/e-coli.

World Health Organization (WHO) (2019). 1 in 3 people globally do not have access to safe water. Retrieved November 24, 2019 from https://www.who.int/news-room/detail/18-06-2019-1-in-3-people-globally-do-not-have-access-to-safe-drinking-water-unicef-who

Wu, W., Wu, W., Ji, S., Guo, H., Wang, X., and Zhao, J. (2011). The synthesis of 5,10,15,20-tetraarylporphyrins and their platinum(II) complexes as luminescent oxygen sensing materials. *Dyes and Pigments*, *89*(3), 199–211.

Xi, C., Zhang, Y., Marrs, C. F., Ye, W., Simon, C., Foxman, B. and Nriagu, J. (2009). Prevalence of Antibiotic Resistance in Drinking Water Treatment and Distribution Systems. *Applied and Environmental Microbiology*, *75*(17), 5714–5718.

Yamaguchi, Y., Matsubara, Y., Ochi, T., Wakamiya, T. and Yoshida Z. (2008). How the π Conjugation Length Affects the Fluorescence Emission Efficiency. *J. Am. Chem. Soc. 130,* 13867–13869.

Yasuyuki, M., Kunihiro, K., Kurissery, S., Kanavillil, N., Sato, Y. and Kikuchi, Y. (2010). Antimicrobial properties of nine pure metals: a laboratory study using *staphylococcus aureus* and *Escherichia coli. Journal of bio-adhesion and biofilm research 26*, 851–858.

Yoder, J., Roberts, V., Craun, G., Hicks, L. and Roy, S. (2008). Surveillance of waterborne diseases and outbreaks associated with Drinking Water and Water not intended for Drinking. United States, 2005–2006. *MMWR Surveilance Summaries 57, 1–9.*

Yoon, I., Li, J. and Shim, Y. (2013). Advance in photosensitizers and Light delivery in photodynamic therapy. *J of clin Endosc 46*(1), 7-23.

Yuan, Q., Guo, M., and Yang, K., (2015). Fate of Antibiotic Resistant Bacteria and Genes during Wastewater Chlorination: Implication for Antibiotic Resistance Control. *PLoS ONE 10*(3), 1-11.

Zhang, A., Kwan, L. and Stillman, M. (2017). The spectroscopic impact of interactions with the four Gouterman orbitals from peripheraldecoration of porphyrins with simple electronwithdrawing and donating groups. *Org. Biomol. Chem, 15*, 9081–9094.

Zheng, W., Shan, N., Yu, L., and Wang, X. (2008). UV visible , fluorescence and EPR properties of porphyrins and metalloporphyrins. *Dyes and Pigments*, *77*, 153–157.

Zoltan, T., Vargus, F. Rivas, C. Perez, J. and Biasutto, A. (2010). Synthesis, Photochemical and Photoinduced Antibacterial Activity Studies of *meso*-Tetra(pyren-1-yl)porphyrin and its Ni, Cu and Zn Complexes. *Sci Pharm., 78,* 767–789.

APPENDICES

Appendix A: Spectral data for H_2TBrPP

Appendix A.1: Mass Spectral Data for H_2TBrPP

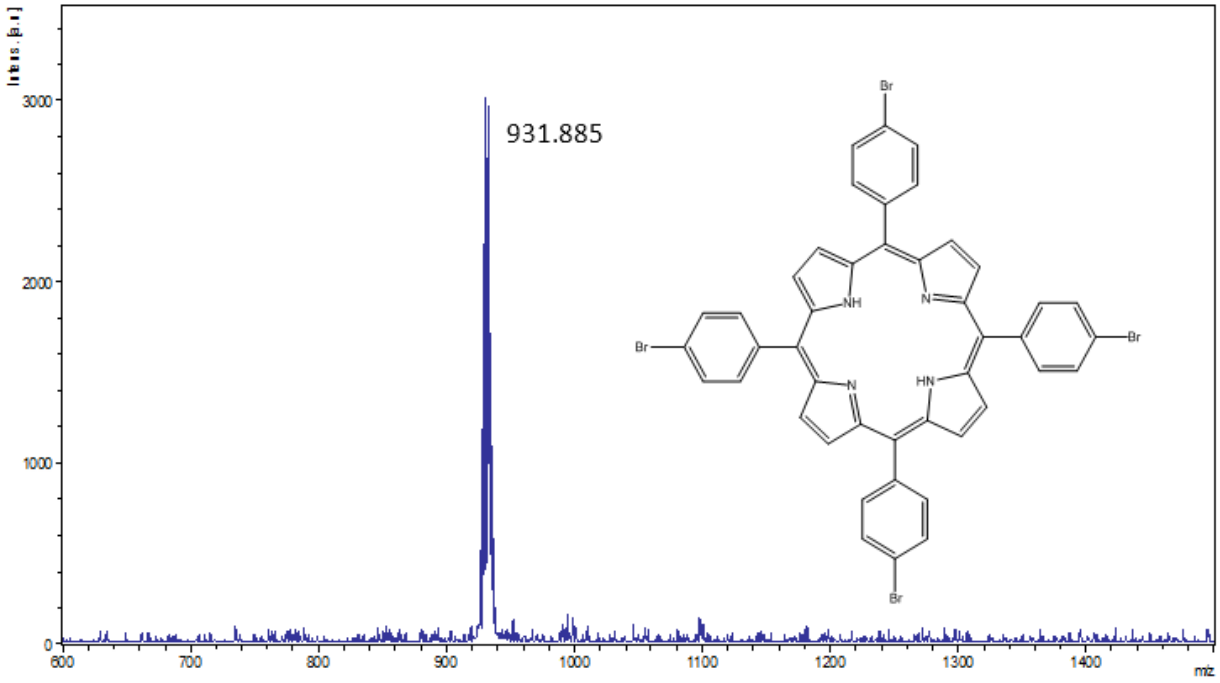

Appendix A.2: ^{1}H NMR Data for H_2TBrPP

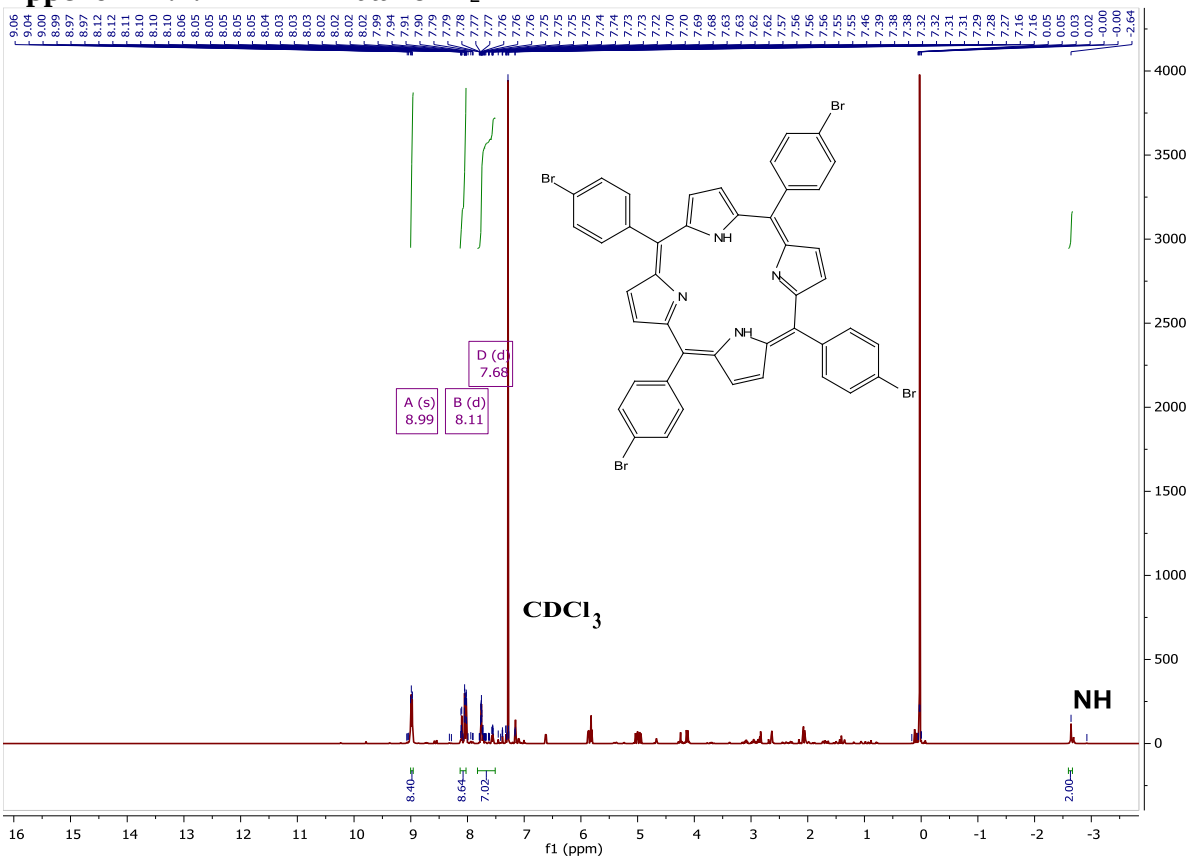

Appendix B: Spectral Data for H_2TPyP

Appendix B.1: Mass Spectral Data for H_2TPyP

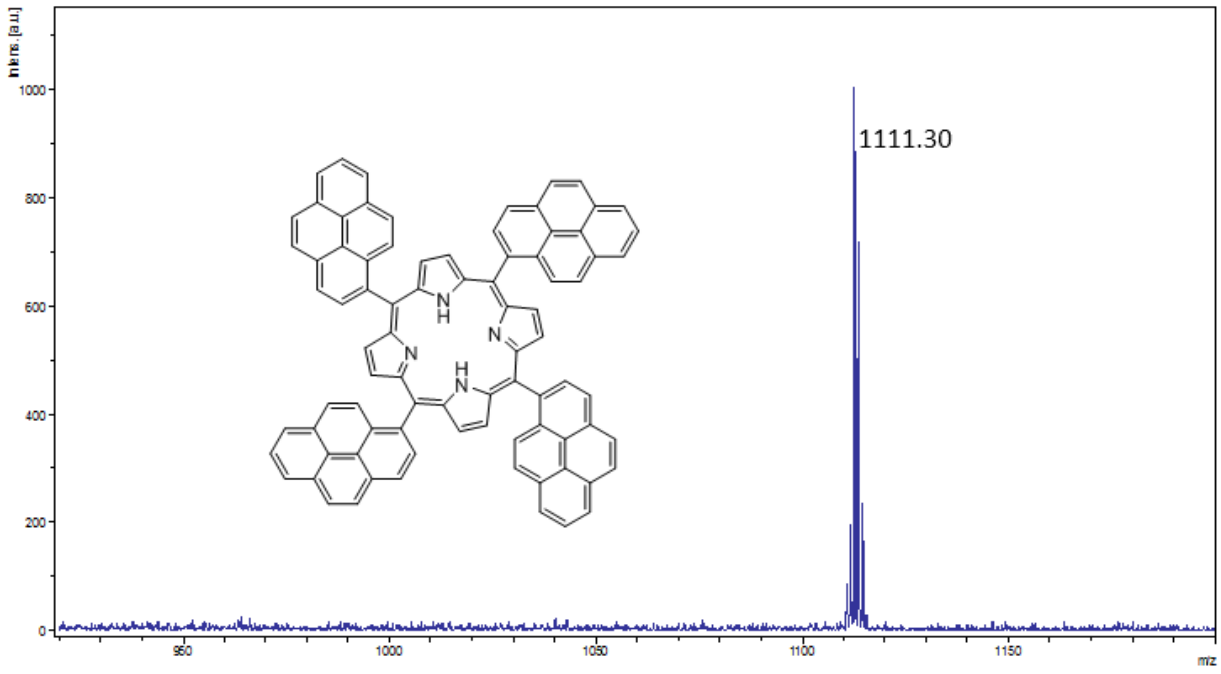

Appendix B.2: ^{1}H NMR Data for H_2TPyP

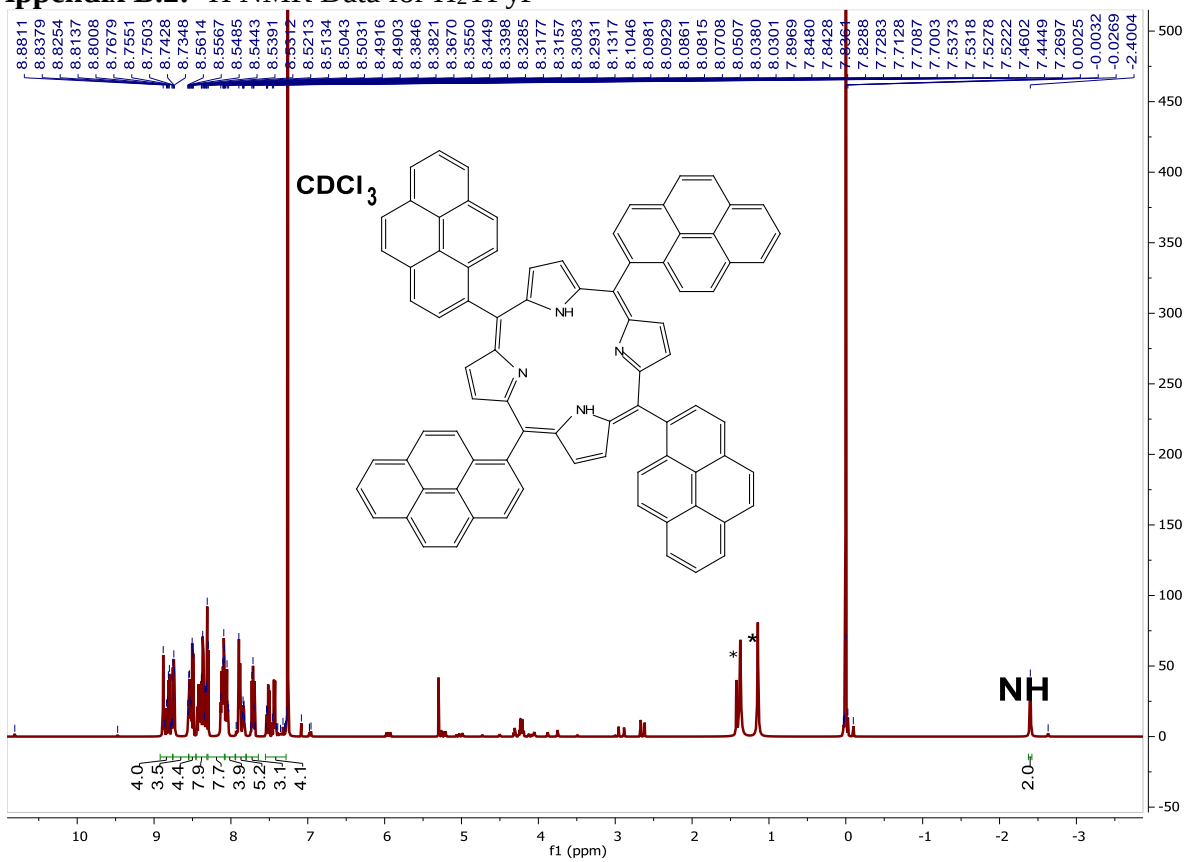

Appendix C: Spectral Data for ZnTPyP

Appendix C.1: Mass Spectral Data for ZnTPyP

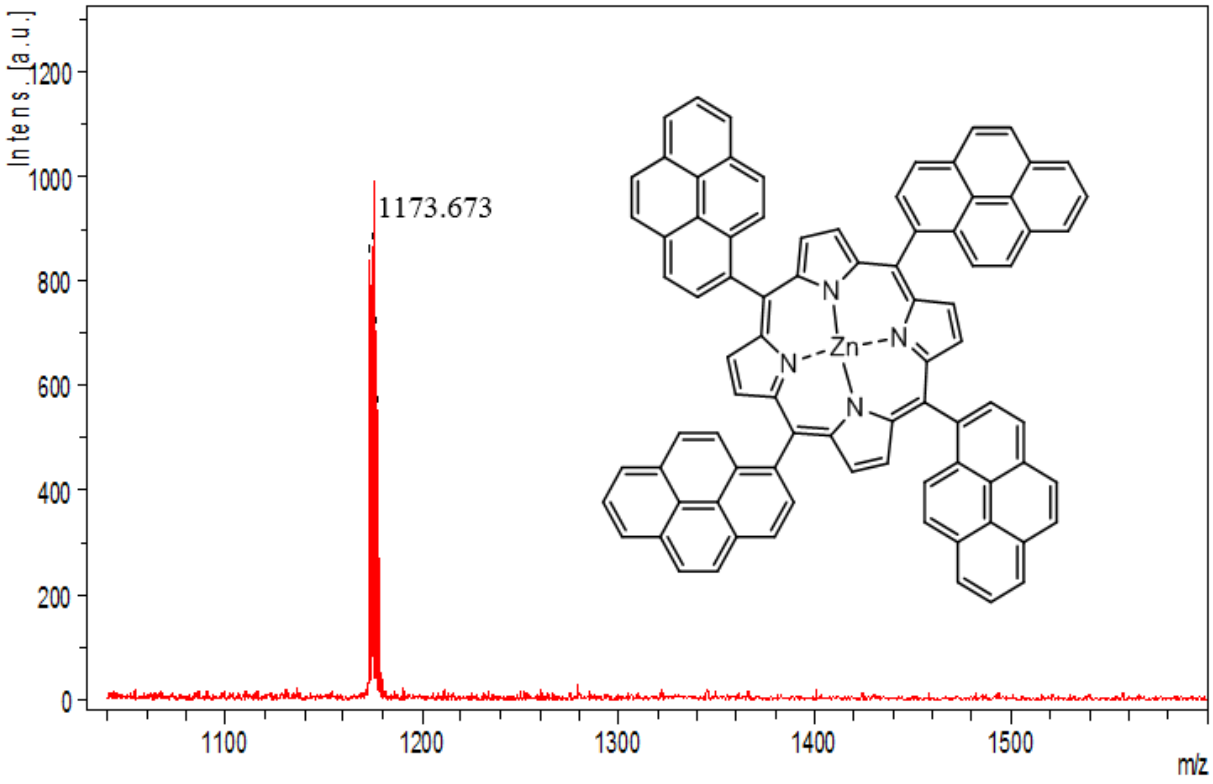

Appendix C.2: ^{1}H NMR Data for ZnTPyP

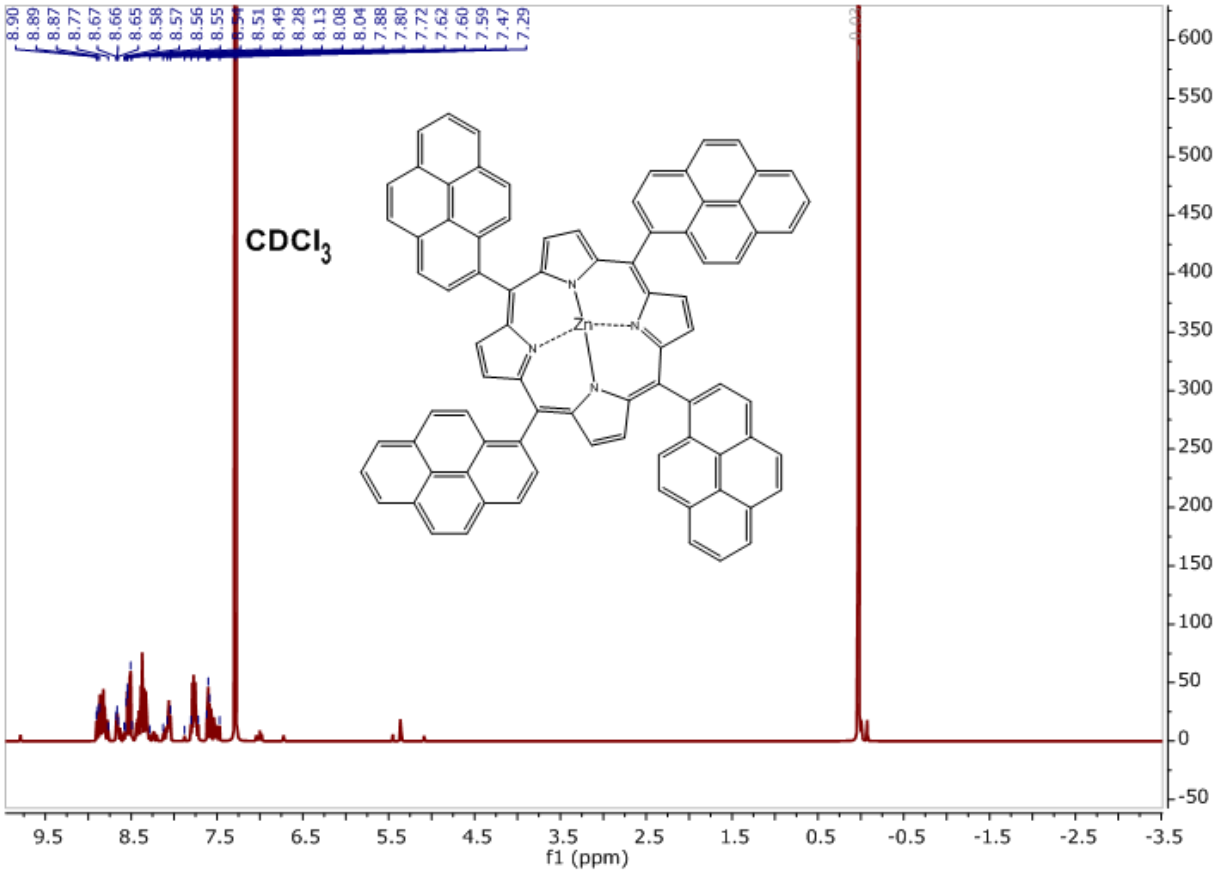

Appendix D: Spectral Data for GaClTPyP

Appendix D.1: Mass Spectral Data for GaClTPyP

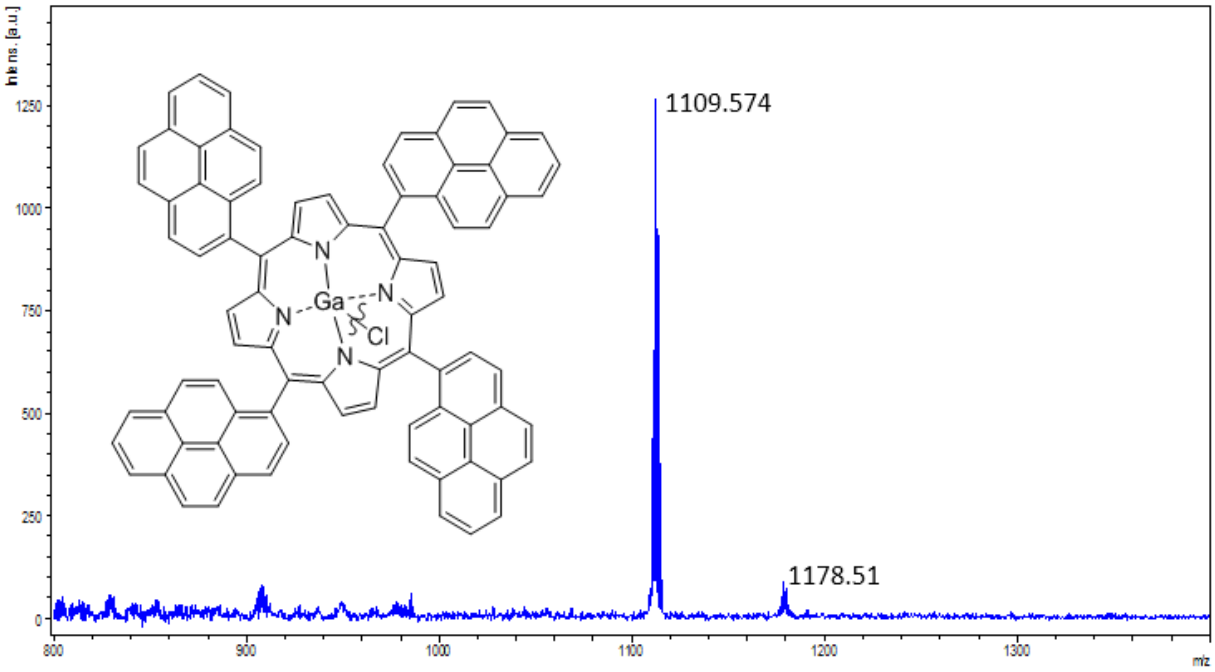

Appendix D.2: ^{1}H NMR Data for GaClTPyP

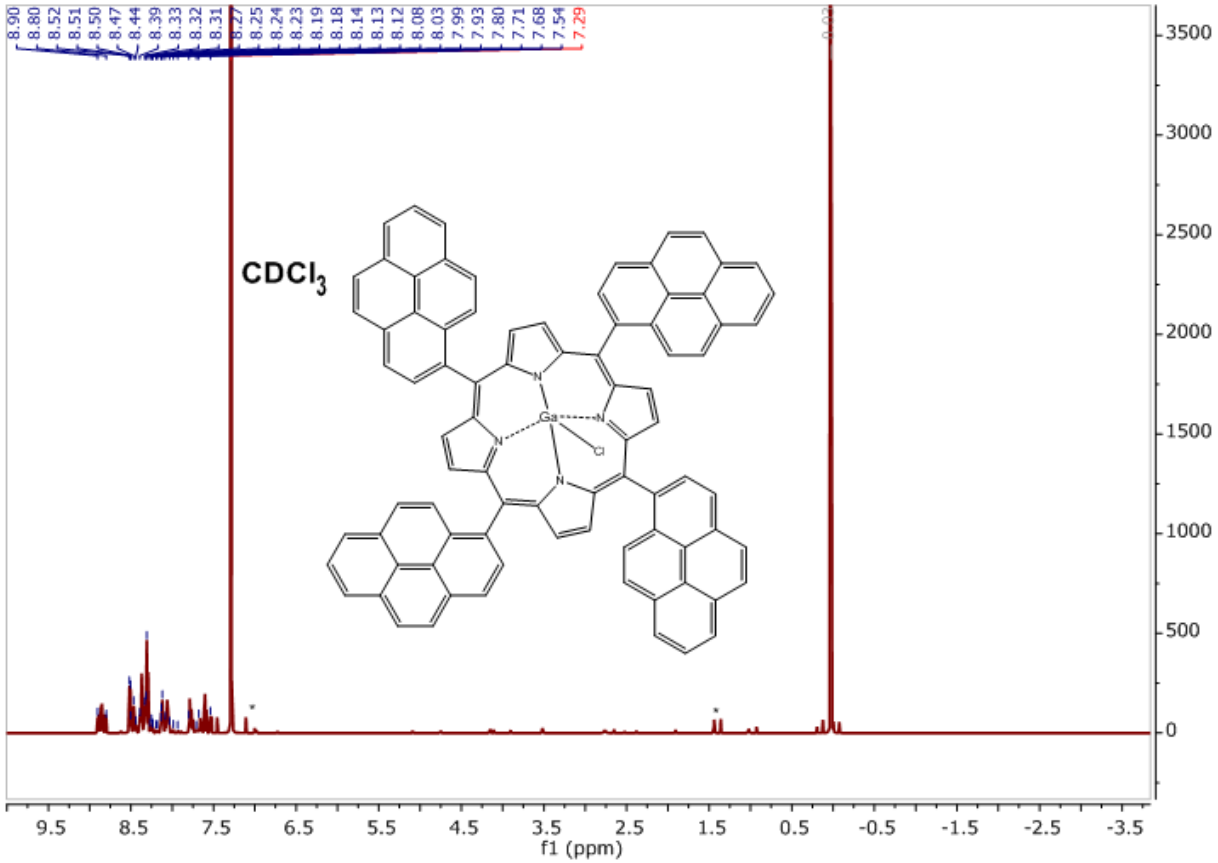

Appendix E: Spectral Data for InClTPyP

Appendix E.1: Mass Spectral Data for InClTPyP

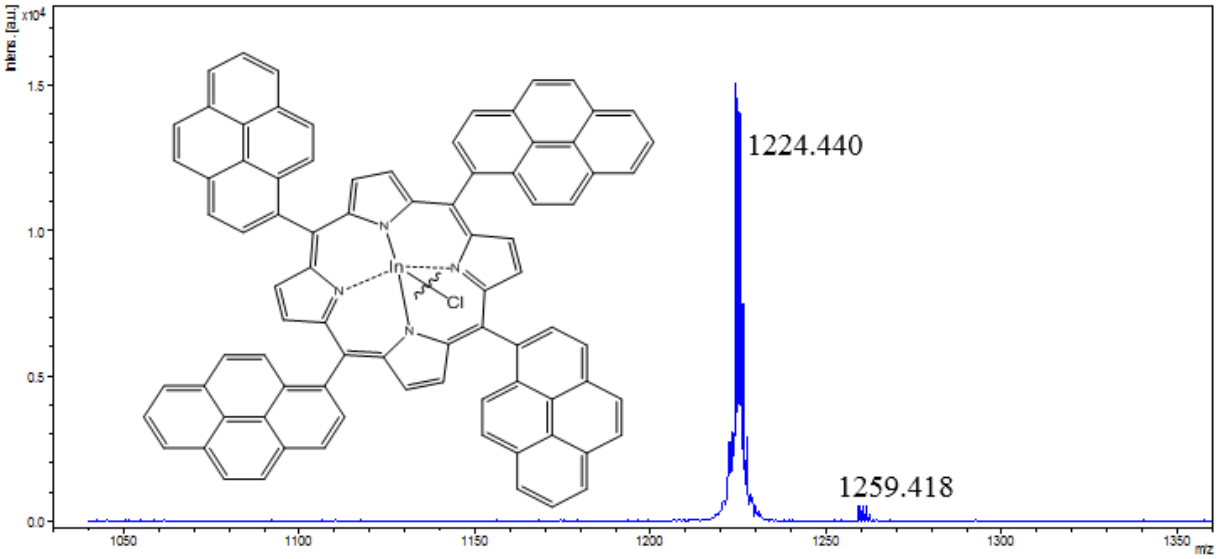

Appendix E.2: ^{1}H NMR Data for InClTPyP